Nanotechnology, Science and Applications

Dovepress
Taylor & Francis Group

Open Access Full Text Article

ORIGINAL RESEARCH

Biometric, Physiological, and Genetic Profile of Chrysanthemum Plants in Response to CdS, Co_3O_4, and Fe_3O_4@Co Nanoparticles Treatment

Alicja Tymoszuk[1], Dariusz Kulus[1], Alicja Kulpińska[1], Katarzyna Gościnna[2], Paulina Pietrzyk-Thel[3], Magdalena Osial[3]

[1]Laboratory of Horticulture and Landscape Architecture, Department of Biotechnology, Faculty of Agriculture and Biotechnology, Bydgoszcz University of Science and Technology, Bydgoszcz, Poland; [2]Department of Agronomy and Food Processing, Faculty of Agriculture and Biotechnology, Bydgoszcz University of Science and Technology, Bydgoszcz, Poland; [3]Department of Theory of Continuous Media and Nanostructures, Institute of Fundamental Technological Research, Polish Academy of Sciences, Warsaw, Poland

Correspondence: Alicja Tymoszuk, Laboratory of Horticulture and Landscape Architecture, Department of Biotechnology, Faculty of Agriculture and Biotechnology, Bydgoszcz University of Science and Technology, Bernardyńska 6, Bydgoszcz, 85-029, Poland, Email alicja.tymoszuk@pbs.edu.pl

Purpose: Chrysanthemum is one of the most popular ornamental plants worldwide. Its breeding remains a highly relevant topic. Nanotechnology significantly and interdisciplinarily contributes to the progress in modern horticulture. To date, there are no studies on the use of the proposed heavy metal-based nanoparticles in mutation breeding of ornamental plants.

Methods: CdS NPs, Co_3O_4 NPs, and Fe_3O_4@Co NPs were synthesized and applied at a concentration of 75 $mg \cdot L^{-1}$ in the in vitro internode culture of *Chrysanthemum* × *morifolium* (Ramat) Hemsl. 'Lilac Wonder'.

Results: The highest number of adventitious shoots was regenerated on the control and Fe_3O_4@Co NP-treated internodes, whereas the use of CdS NPs and Co_3O_4 NPs hampered regeneration. The NP-treated shoots, compared to the control, accumulated less flavonols and more anthocyanins and polyphenols, and exhibited increased antioxidant capacity. The highest activity of oxidative stress enzymes and the lowest chlorophyll content were noted in CdS NP-treated shoots. The tested nanoparticles also affected the further growth and development of plants during ex vitro greenhouse cultivation. The longest stems were found in Fe_3O_4@Co NP-treated plants, contrary to CdS NPs and Co_3O_4 NPs. The CdS NP-treated plants developed leaves with the smallest surface area, perimeter, length, and width. Evaluation of inflorescences revealed quantitative changes in anthocyanins content. The highest pigment content was found in ligulate flowers of Fe_3O_4@Co NP-treated plants. One individual with variegated leaves was phenotypically identified within Co_3O_4 NP-treated plants. Genetic variation was detected in 7–8.1% of the plants studied. The SCoT marker system generated more bands and polymorphisms than RAPD. PCoA analysis revealed distinct genetic groupings, with the most altered genotype (treated with CdS NPs) classified as polymorphic by both marker systems. The other 11 polymorphic genotypes did not overlap between RAPD and SCoT analyses.

Conclusion: Our results proved that nanoparticles can serve as a novel and valuable tool for plant breeding.

Keywords: breeding, *Chrysanthemum* × *morifolium*, genetic marker, nanobiotechnology, phenotype, physiology

Introduction

In recent years, the convergence of nanotechnology and biotechnology in plant science has begun a new area of exploration, enabling unprecedented insights into the intricacies of plant growth and development.[1] Nanoparticles (NPs) are defined as atomic or molecular aggregates less than 100 nm in size, possessing unique and captivating physical and chemical properties compared to micrometer-sized materials. Nanoparticles, due to their small size, increased number of surface atoms, huge surface area-to-volume ratio, high particle energy, and catalytic reactivity, easily interact with biological systems, eg, plant cells.[2–4] Interactions between nanoparticles and living organisms are complex and often ambiguous. The same type of nanoparticles can cause different biological effects depending on the genotype, organ, age and developmental stage of the plant, cultivation conditions, time of exposure to nanoparticles, and depending on the

Received: 19 August 2025
Accepted: 4 November 2025
Published: 5 December 2025

physicochemical properties of nanoparticles, including their composition, functional groups on the surface, type of coating, concentration, size, shape, stability or method of plant treatment.[5–7]

The application of nanotechnology in agriculture has greatly improved plant protection and nutrition, and significantly increased efficiency and productivity. Research in the realm of horticultural plants is still in its early stages. Among other applications, the effects of nanoparticles on in vitro plant regeneration have emerged as a fascinating area of study.[1,3] A review of scientific publications provides reports on the positive aspects of using various nanoparticles in plant in vitro cultures – most often for eliminating microbiological contamination, stimulating seed germination and seedling development, inducing caulogenesis, organogenesis and somatic embryogenesis, or producing metabolites. Nanoparticles can also negatively affect plant metabolism, growth, and development.[8,9] It is assumed that nanoparticles modify structural elements of cell membranes and cellular macromolecules, affect cell division, induce oxidative stress, and disrupt physiological and biochemical processes of plants.[10,11]

The genotoxicity of nanoparticles has been especially studied in microbes and mammals, while it is little examined in plants. It has been proven that nanoparticles can induce genotoxicity either directly or indirectly. In the direct mechanism, nanoparticles pass through the cell and nuclear membrane and interact with DNA mechanically or chemically. Indirect genotoxicity of nanoparticles results from interaction with proteins (involved in replication, transcription, translation, etc) or induction of oxidative stress, which plays a critical role in nanotoxicity. Nanoparticle treatment induces chromosomal aberrations, affects the cell cycle and DNA repairing system, alters gene expression, causes DNA damage, and leads to epigenetic variations in the plant genome.[12,13] The 10, 20, 40, and 50 $mg \cdot L^{-1}$ Ag NPs treated root tip cells of wheat (*Triticum aestivum* L.) exhibited various types of chromosomal aberrations, such as incorrect orientation at metaphase, chromosomal breakage, metaphasic plate distortion, spindle dysfunction, stickiness, aberrant movement at metaphase, fragmentation, scattering, unequal separation, chromosomal gaps, multipolar anaphase, erosion, as well as distributed and lagging chromosomes.[14] Molecular markers can also be used to detect the nanoparticles' effect on the plant genome and to determine potential mutations in the DNA sequence.[15]

Chrysanthemum × *morifolium* (Ramat.) Hemsl. (formerly *Chrysanthemum* × *grandiflorum* /Ramat./ Kitam.) (Asteraceae) is one of the most culturally and economically important ornamental plant species in the world.[16,17] The value of its inflorescence is primarily determined by the ligulate flowers, which exhibit a wide variety of colors and shapes. Inflorescences also contain biologically active metabolites and are a herbal material.[18] The demand for cultivars with new inflorescence and/or leaf features, increased stress tolerance, or diversified plant habit is growing year by year. Moreover, improvements in large-scale cuttings production with the use of micropropagation are also of great importance.[19]

Exploring the genotoxic effects of nanoparticles on plants is particularly valuable for the development of breeding methods. The novelty and originality of our study lie in synthesizing potentially toxic and mutagenic metal-sulfide-based (CdS) and metal oxide-based (Co_3O_4 and Fe_3O_4@Co) nanoparticles and using them to induce molecular and phenotypic variability in chrysanthemum. Novel, user-friendly, easily accessible, and moderately expensive techniques of plant improvement are desirable. It is crucial for ornamental plants due to the huge market demand for new cultivars. So far, only the usefulness of silver nanoparticles (Ag NPs) in chrysanthemum breeding has been demonstrated.[20,21] Against, zinc oxide nanoparticles (ZnO NPs) and zinc oxide nanoparticles combined with silver nanoparticles were successfully used to improve the efficiency of adventitious shoots regeneration,[22] and biometric parameters of chrysanthemum shoots and/or roots in meristematic explant cultures.[23]

Cadmium sulfide nanoparticles (CdS NPs) have proven biomedical properties and are popular in biosensors, bioimaging, antibacterial, and anticancer applications.[24] Ullah et al[25] applied CdS NPs (3–100 $mg \cdot L^{-1}$) on maize (*Zea mays* L.) seedlings, and observed chlorotic effects, metabolic disruption, as well as reduced shoot and root biomass. In plants, cadmium toxicity causes oxidative stress, destruction of cell membranes, biomolecules, and organelles. Cd also reduces uptake of Fe and Zn, resulting in leaf chlorosis, and interferes with the transport and uptake of Ca, P, Mg, K, and Mn.[26] Excessive concentrations of sulfur also harm plants, damaging the root system, foliage, and reducing growth.[27]

Cobalt (Co) is one of the toxic metals for plants. When its level increases, it leads to severe toxicity. Cobalt stress inhibits plant growth and development through oxidative stress. It also reduces nutrient uptake and photosynthetic efficiency.[28] Cobalt oxide nanoparticles (Co_3O_4 NPs) are used in wastewater treatment, drug delivery, magnetic

resonance imaging, electrochromic sensors, heterogeneous catalysis, and energy storage devices.[2,29] They also have various biomedical applications due to distinctive antioxidant, antimicrobial, antifungal, larvicidal, antileishmanial, and anticholinergic properties.[30] In the study conducted by Ogunyemi et al.[31] Co_3O_4 NPs improved the agronomic parameters and biomass of rice (*Oryza sativa* L.) and increased the photosynthetic parameters of *Arabidopsis thaliana* (L.) Heynh. In rapeseed (*Brassica napus* L.), Co_3O_4 NPs applied at low concentrations stimulated growth; however, high concentrations caused extensive oxidative damage and mediated defense responses.[32] Faisal et al[33] reported genotoxic effects of cobalt oxide nanoparticles on eggplant (*Solanum melongena* L).

Iron oxide nanoparticles (Fe_3O_4 NPs) are one of the most widely explored nanomaterials. Due to their unique properties (superparamagnetism, inherent biocompatibility), they have found numerous applications in medical diagnostics, controlled drug release, separation technologies, and environmental engineering.[34] Fe_3O_4 NPs promoted growth and chlorophyll accumulation in muskmelon (*Cucumis melo* L.)[35] or increased chlorophyll content and vegetative growth of chrysanthemum plants in greenhouse experiments.[36] Bare and citrate-stabilized (CA) iron oxide nanoparticles affected the germination and growth of chrysanthemum 'Richmond' propagated from synthetic seeds.[37] In this approach, nanoparticles in combination with indole acetic acid (IAA) were added to the alginate bead matrix containing a single axillary bud. It was found that shorter exposure to Fe_3O_4CA stimulated the elongation of shoots in vitro and improved the acclimatization efficiency of plants in the greenhouse, resulting in improved leaf growth metrics. Negative effects were evident after extended exposure. Therefore, it is interesting to explore the effects of other nanoparticle types, not only for reproduction purposes but also for mutation breeding, and to study other cultivars. The excess of iron ions in plants can cause oxidative stress, damage to membranes, lipids, proteins, and DNA, stunted growth, reduced root development, decreased water and nutrient uptake, and reduced photosynthetic activity.[38] To date, there are no studies on the use of the proposed heavy metal-based nanoparticles in mutation breeding of ornamental plants. Importantly, in addition to the well-known toxicity of heavy metal ions to plants, CdS, Co_3O_4, and Fe_3O_4@Co nanoparticles possess semiconducting properties that enable them to generate reactive oxygen species (ROS).[39–41] These, in turn, directly affect plant physiology by increasing oxidative stress.

Undoubtedly, interactions between nanoparticles and plants require further detailed research to better understand and use the potential that nanotechnology offers to modern agriculture and horticulture. The specific objectives of our study focused on: (1) synthesis and physicochemical characteristic of CdS, Co_3O_4, and cobalt doped Fe_3O_4 (Fe_3O_4@Co) NPs, (2) establishment of chrysanthemum in vitro cultures and treatment of internode explants with nanoparticles, (3) determination of the efficiency of in vitro adventitious shoot regeneration, (4) assessment of the extent of oxidative stress by analyzing the biochemical profile (pigment content, chlorophyll fluorescence, antioxidant capacity, and enzymatic activity) of plant tissues in vitro, (5) phenotype and genetic analyses of plants at the stage of ex vitro cultivation in the glasshouse; to further reveal effects of these nanoparticles on plants and study their use in plant mutation breeding. The research hypothesis assumed that selected types of nanoparticles can penetrate plant cells and induce changes at the physiological and molecular level, and the resulting genetic variability among regenerated plants can manifest in their phenotype and be valuable for breeding. The use of nanoparticles as a chemical mutagen added to the micropropagation medium can make chrysanthemum breeding relatively easy and effective. Therefore, it could be routinely performed in in vitro plant laboratories, without the need for specialist equipment or the use of expensive and advanced methods of genetic transformation and genome editing.

Materials and Methods

Chemicals and Methods for Nanoparticles

Cobalt (II) chloride hexahydrate ($CoCl_2.6H_2O$), iron (II) chloride tetrahydrate ($FeCl_2.4H_2O$), iron (III) chloride hexahydrate ($FeCl_3.6H_2O$), and sodium hydroxide (NaOH) were supplied from the Warchem Sp. z o.o., Warsaw, Poland. Cadmium acetate ($Cd(CH_3COO)_2.2H_2O$), sodium sulfide nonahydrate ($Na_2S{\cdot}9H_2O$), and sodium borohydride ($NaBH_4$) were supplied from Sigma-Aldrich, St. Louis, MO, USA. All the chemicals were used without further purification. Ethanol (EtOH) and hydrochloric acid (HCl) were purchased from POCH, Gliwice, Poland. Deionized (DI) water was obtained using the HYDROLAB water filtering system, Gliwice, Poland.

The morphology of nanoparticles was studied using Scanning Electron Microscopy (SEM), Merlin Zeiss, Carl Zeiss, Stuttgart, Germany, where the dried samples were placed on the conducting tape. The Attenuated Total Reflection Fourier Transform Infrared Spectroscopy (ATR-FTIR) was used to record the spectra in the 4000–400 cm^{-1} infrared region that are characteristic of the specific vibrations in the obtained particles. Before the spectra recording, the samples were ground with a mortar and pestle. ATR-FTIR Spectrum Two Perkin Elmer was supplied by Pro-Environment Polska Sp. z o.o., Warsaw, Poland. The dynamic light scattering (DLS) method was used to measure the hydrodynamic size of the particles with Malvern Instruments Zetasizer Nano Sizer, Malvern, UK. The measurements were performed in the aqueous solution at pH 5.8, which is identical to the following in vitro conditions.

Procedures for Nanoparticles

Synthesis of CdS NPs

Two hundred and sixty-six milligrams of $Cd(CH_3COO)_2$ was dissolved in the 100 mL of 1:1 water-ethanol solution by magnetic stirring at 600 rpm at 80°C. Then, 240 mg of Na_2S was dissolved in 1:1 water-ethanol and added dropwise with continuous stirring and heating for 15 min. After the synthesis, the solution was cooled and washed several times with DI water and EtOH, with centrifuging. Last, the precipitate was dried overnight at 50°C.

Synthesis of Co_3O_4 NPs

First, 450 mg of $CoCl_2.6H_2O$ was placed into a 50 mL beaker, where 20 mL of EtOH was added, and the solution was stirred with a magnetic stirrer at 600 rpm for 5 min at room temperature. Next, 500 mg of $NaBH_4$ was added with continuous stirring for 15 min, until the change in the color of the solution from blue to black. After synthesis, the powder was rinsed several times with water (min. 5 times) to remove excessive $NaBH_4$, and centrifuged at 4000 rpm for 4.5 min. Blackish precipitate was rinsed with EtOH twice and dried onto a Petri dish at 90°C for 60 min.

Synthesis of Fe_3O_4@Co NPs

To prepare the Co-doped Fe_3O_4 (labeled as Fe_3O_4@Co), 540 mg of $FeCl_36H_2O$, 100 mg of $FeCl_24H_2O$, and 100 mg of $CoCl_26H_2O$ were placed in a 50 mL volume beaker and dissolved in 20 mL of DI by a magnetic stirrer with a mixing rate of about 600 rpm. Next, the 1 M NaOH solution was added dropwise till pH 10.5 with controlled stirring at 600 rpm at 85°C for 15 min. Next, the suspension was cooled down, the precipitate was collected at the bottom of the beaker onto the magnet, and washed several times with DI water and EtOH by centrifuging. Next, the samples for analysis were dried in an oven overnight at 50°C.

Characteristics of Nanoparticles

Figure 1a clearly shows the formation of CdS granules sized ~50 nm. Following, Co_3O_4 also forms aggregates by the granules having a similar size (Figure 1b), while the cobalt-doped iron oxide Fe_3O_4@Co spherical nanoparticles are sized below 20 nm in diameter (Figure 1c).

Complementary to the SEM analysis, the DLS method was used to determine the hydrodynamic diameter d_H. Figure 1d presents d_H for CdS above 150 nm, which can relate to the agglomerates or aggregates formation, while the d_H values decrease for the Co_3O_4 ~125 nm and below 100 nm for the Fe_3O_4@Co, which are in good agreement with the SEM results for the dry samples.

Subsequently, the presence of characteristic vibrations in the nanoparticles was studied using ATR-FTIR. As can be seen in the green curve in Figure 1e, the Co-O vibrations confirm the presence of cobalt oxide, where the band at 583 cm^{-1} Co-O relates to the Co^{2+}-O vibration in tetrahedral sites. The following band at 657 cm^{-1} is the stretching vibration of Co^{3+}-O in the octahedral sites in the spinel lattice.[42] The weak band at 505 cm^{-1} can be associated with the $Co^{2+}O_6$ vibration that can suggest the formation of a non-stoichiometric structure for the unreduced Co^{3+} ions in the cobalt oxide structure.[43] The minor band at 1254 cm^{-1} can relate to the CO_2 residues adsorbed onto the nanoparticles, while the following band at 1350 cm^{-1} can be ascribed to the C-O stretching vibration from the ethanol residues. The following band at 1636 cm^{-1} can correspond to the H-O-H bending vibration of water molecules and/or ethanol.

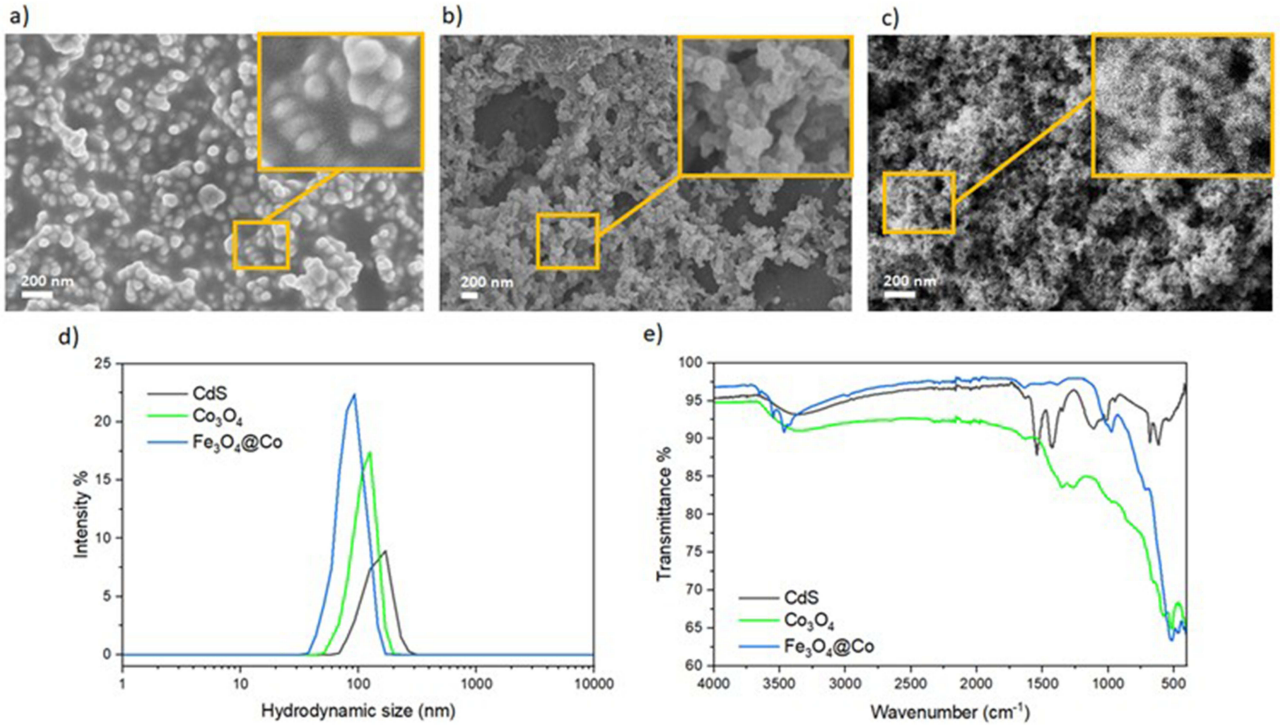

Figure 1 Scanning Electron Microscopy (SEM) images of (**a**) CdS NPs, (**b**) Co_3O_4 NPs, (**c**) Fe_3O_4@Co NPs, (**d**) hydrodynamic diameter, and (**e**) Fourier Transform Infrared (FTIR) spectra for CdS, Co_3O_4, and Fe_3O_4@Co NPs.

The blue curve in Figure 1e is characteristic of the iron oxide doped with cobalt. The minor band located at 421 cm^{-1} appears for the Fe-O vibrations in the octahedral sites, while the vibrations at 471 cm^{-1} and 522 cm^{-1} come from the Fe-O in the tetrahedral sites of spinel structure.[44] The following band at 713 cm^{-1} is characteristic of the Co-O in the iron oxide doped with cobalt.[45] The bands at 974 cm^{-1} and 1013 cm^{-1} can come from the organic residues from the sample washing, while bands at 1379^{-1} and 1639 cm^{-1} are characteristic of the C-O and water, respectively.

The black curve presents the spectrum recorded for CdS, where the bands at 613 cm^{-1} and 685 cm^{-1} are characteristic of the CdS stretching vibration,[46] while minor bands at 539 cm^{-1} may relate to the S-S[47] or surface oxidation.[48] The following bands in the range between 950 cm^{-1} and 1110 cm^{-1} can be attributed to the carboxylates in the sample from the cadmium precursor. Next, bands at 1345 cm^{-1}, 1425 cm^{-1}, and 1542 cm^{-1} can be ascribed to the C-O, C=O, and H-O-H stretching, respectively. The presence of the broad band in all samples above 3400 cm^{-1} is caused by the O-H vibrations.[49]

In vitro Culture Establishment and Nanoparticle Treatments

Chrysanthemum × *morifolium* (Ramat). Hemsl. 'Lilac Wonder' was used in the experiment. The plant material was obtained from the in vitro gene bank of the Laboratory of Horticulture and Landscape Architecture, Bydgoszcz University of Science and Technology, Bydgoszcz, Poland. The plants were identified and authenticated by Dr Tomasz Stosik, a member of the Polish Botanical Society (PBS). A voucher specimen (no. 1594a) was deposited in the Herbarium of the Department of Plant Microbiology and Ecology, Bydgoszcz University of Science and Technology, Bydgoszcz, Poland.

Internode explants were inoculated on the modified MS medium,[50] in which the content of calcium and iron was increased by half, 30 $g \cdot L^{-1}$ sucrose, and 8 $g \cdot L^{-1}$ Plant Propagation LAB-AGAR™ (BIOCORP, Warsaw, Poland) were added. The medium was supplemented with plant growth regulators: 0.6 $mg \cdot L^{-1}$ BAP (6-benzylaminopurine) and 2.0 $mg \cdot L^{-1}$ IAA (indole-3-acetic acid) (Sigma-Aldrich, St. Louis, MO, USA) to induce adventitious organogenesis.

https://doi.org/10.2147/NSA.S557241

The pH was adjusted to 5.8, and next, 40 mL of the medium was poured into 350 mL glass jars sealed with plastic and autoclaved at 105 kPa and 121°C for 20 min.

Four internode explants were placed, in a horizontal position, in each culture jar. The nanoparticles suspensions: CdS, Co_3O_4, or Fe_3O_4@Co NPs, at the concentration of 75 mg·L^{-1} were sterilized in an autoclave, and, before application, placed for 30 min in the Elmasonic S80(H) Ultrasonic Cleaner with the ultrasonic frequency of 37 kHz and the effective ultrasonic power of 150 W (Elma Schmidbauer GmbH, Singen, Germany) to disassemble potential aggregates. Then, nanoparticle suspensions were poured onto the explants and culture medium with an automatic pipette, 2 mL of each suspension per culture jar. The concentration of nanoparticles suspensions was determined based on the results of our previous research on chrysanthemum breeding.[21] Explants inoculated on the medium without nanoparticles were used as the control object. Each experimental object consisted of 15 jars (60 explants in total). After eight culture weeks, the share of explants regenerating adventitious shoots, and the mean number of adventitious shoots per inoculated explant were estimated. Biochemical analysis was performed as described in detail below. Shoots were cut off from explants and transferred to the modified MS rooting medium with 2.0 mg·L^{-1} IAA for two weeks. Additionally, 20 shoots propagated via the single-node method on the MS medium without PGRs and NPs were also rooted as a genotype/phenotype standard of 'Lilac Wonder' chrysanthemum. Rooted plantlets were then cultivated ex vitro in a greenhouse.

In vitro cultures were maintained in the growth room with the following conditions: 23±1°C, 16/8 h light/dark photoperiod, photosynthetic photon flux density of 35 μmol·m^{-2}·s^{-1} (Philips TLD 36W/54 fluorescent lamps emitting cool daylight; Koninklijke Philips Electronics N.V., Eindhoven, the Netherlands).

Biochemical Activity of in vitro Regenerated Plants

Pigments and Chlorophyll Fluorescence

The relative contents of flavonols, anthocyanins, chlorophyll, and Soil Plant Analysis Development (SPAD) leaf greenness index in the fresh leaves were estimated in 80 plants per experimental treatment using a portable MPM-100 multipigment meter (Opti-Sciences Inc., Hudson, NH, USA). The relative values of F_0 (minimal fluorescence), F_V (variable fluorescence), F_M (maximal fluorescence), F_V/F_M and F_V/F_0 ratios in the leaves were measured in 40 plants per experimental treatment using the OS-30p+ chlorophyll fluorimeter (Opti-Sciences Inc., Hudson, NH, USA).

Enzyme Activity

To determine the enzymatic activity, fresh leaves (100 mg) were homogenized in phosphate buffer (100 mM; pH 7.4) with 1 mM EDTA, 1 mM dithiothreitol (DTT), and 2% (w/v) polyvinylpyrrolidone (PVP) according to Homaee and Ehsanpour.[51] The homogenates were next centrifuged (13,000× g for 20 min at 4°C; Centrifuge MPW-260R, MPW MED INSTRUMENTS, Warsaw, Poland). Supernatants were used for the determination of the total protein content[52] and the activities of ascorbate peroxidase (APOX; EC 1.11.1.11),[53] guaiacol peroxidase (GPOX; EC 1.11.1.7),[54,55] and superoxide dismutase (SOD; EC 1.15.1.1).[56] The spectrophotometric analyses were performed using the SmartSpec PlusTM spectrophotometer (BioRad, Hercules, CA, USA) at specific wavelengths: for proteins at 595 nm, for APOX at 265 nm, for GPOX at 430 nm, and for SOD at 560 nm. Measurements were repeated six times for each experimental treatment. The enzymatic activity U (μmol·min^{-1}) was calculated per 1 mg of total protein content.

Total Content of Polyphenols (TCP) and Antioxidant Capacity – Ferric Reducing Antioxidant Power (FRAP) and [2,2'-Azino-Bis(3-Ethylbenzothiazoline-6-Sulfonic Acid)] Assay (ABTS)

Fresh plant tissue samples were put in zip-lock foil bags, frozen, and stored at −20°C for 24 h (AFG 6402 E-B freezer, Whirlpool, Milan, Italy). Next, the material was lyophilized (Alpha 1–4 LSC, Martin Christ Gefriertrocknungsanlagen GmbH, Osterode am Harz, Germany) (moisture content <2%), and ground in a mill into a fine powder (0.3–0.5 mm) (Ultra-Centrifuge Retsch ZM 100, Retsch, Haan, Germany). The prepared samples were stored in the dark in air-tight bags in desiccators. For extraction, a 0.5 g sample was mixed with 30 mL of a methanol-water mixture (70:30 v/v), followed by shaking for 1 h (KS 130 basic shaker, IKA, Staufen im Breisgau, Germany). Next, the samples were centrifuged for 15 min, 3000 rpm, 4°C (ROTINA 420R centrifuge, Hettich, Tuttlingen, Germany). The resulting solution was decanted into a 100 mL flask. This procedure was repeated three times for each experimental treatment. Next, the flask was filled with the methanol-water mixture and mixed to obtain the final extract for the analyses.

The TCP was determined according to Keutgen and Pawelzik.[57] Absorbance was measured using the Shimadzu UV-1800 spectrophotometer (Shimadzu, Kyoto, Japan) at 735.5 nm. Results were calculated based on a calibration curve for gallic acid equivalent (GAE) and given as $mg \cdot g^{-1}$ dry weight (DW), in four repetitions for each experimental treatment.

The FRAP was determined following the Benzie and Strain[58] protocol. A working FRAP solution was prepared by mixing 250 mL of acetate buffer (pH 3.6), 25 mL of a TPTZ (2,4,6-tripyridyl-s-triazine) solution (10 mM in 40 mM HCl), 25 mL of a hexahydrate iron (III) chloride solution (20 mM), and 30 mL of distilled water, at 37°C. A 0.1 mL sample of the plant extract was combined with 1 mL of the working FRAP solution and incubated in a water bath at 37°C for 4 min. Next, the mixture was cooled to room temperature, and absorbance was measured using a UV-1800 spectrophotometer at 593 nm. Measurements were repeated four times for each experimental treatment, and results were expressed in mg TEAC (trolox equivalent antioxidant capacity)$\cdot g^{-1}$ DW.

The antioxidant capacity was determined using the ABTS radical cation method.[59] The ABTS radical cation was generated by incubating a mixture of 7 mM ABTS solution and 2.45 mM $K_2S_2O_8$ in a 1:0.5 ratio in the dark for 12 h. Immediately before measurement, the ABTS radical cation solution was diluted with phosphate buffer (PBS, pH 7.4) until an absorbance of 0.700 (±0.020) was achieved at a wavelength of 734 nm. Subsequently, 0.1 mL of the suitably diluted extract or standard solution was mixed with 3.9 mL of the ABTS working solution and kept in the dark at room temperature for 6 min. Next, absorbance was measured at 734 nm using the Shimadzu UV-1800 spectrophotometer. The rate of ABTS radical cation reduction for each sample was calculated using the equation: Inhibition rate = $(A_{ref} - A_{sample}) / A_{ref} \times 100\%$ (A_{ref} and A_{sample} are the absorbance values for the standard sample and extract, respectively). EC_{50} (expressed in $mg \cdot mL^{-1}$), indicating the concentration required to inhibit 50% of the ABTS radical, was used to evaluate the activity of each sample. Each measurement was repeated four times for each experimental treatment.

All chemical reagents were provided by PHU Syl-Chem Sylwia Kunca, Bydgoszcz, Poland.

Phenotype and Genetic Variability Evaluation During Ex Vitro Plant Cultivation

The rooted plantlets were acclimatized to glasshouse conditions (42°9'6.768" N, 18°0'29.27195" E), in July under natural light conditions. They were planted in plastic multi-trays with a mixture of peat substrate (Hartman, Poznań, Poland) and perlite (Perlit, Šenov u Nového Jičína, Czech Republic) (2:1, v/v). Plants were sprayed with water and covered with perforated transparent foil. The acclimatization lasted two weeks. Next, the plants were planted into plastic pots (ø 29 cm, 10 L, five plants per pot) filled with peat substrate. Plants were cultivated vegetatively in 16 h long-day conditions until mid-October. Subsequently, cultivation was conducted in 10 h short-day conditions to induce generative development. Chrysanthemums were cultivated using the standard method, ie, to form plants with one stem and one inflorescence.

At the stage of full flowering, the plants were assessed by defining the color and shape of the inflorescences. The color of the inner and outer sides of ligulate flowers was established using the Royal Horticultural Society Colour Chart catalog (RHSCC).[60] Moreover, the analysis of anthocyanins content in ligulate flowers was performed. Total anthocyanins (with cyanidin-3-glucoside used as standard) were extracted according to Harborne[61] protocol, in six repetitions for each experimental treatment, and expressed in $mg \cdot g^{-1}$ fresh weight (FW). Stem height (cm) and number of leaves on the stem were also measured. Moreover, excised leaves (three per each plant taken form the lower, middle and upper part of the stem) were scanned (Epson Perfection V800 scanner, Suwa, Japan), and analyzed using imaging software WinFOLIA™ (Reagen Instruments, Quebec, Canada) to measure the leaf area (cm^2), leaf perimeter (cm), leaf length (L) (cm), leaf width (W) (cm), and leaf aspect ratio (W/L).

Randomly Amplified Polymorphic DNA (RAPD)[62] and Start Codon Targeted Polymorphism (SCoT)[63] marker systems were used for genetic analysis (8 RAPD and 8 SCoT primers; Genomed S.A., Warsaw, Poland). A total of 20 plants from each experimental object (control, CdS NPs, Co_3O_4 NPs, and Fe_3O_4@Co NPs) and six genotype/phenotype standard plants were included in each primer analysis. Total genomic DNA was extracted from fresh leaves using the Auto-Pure Mini device for automatic magnetic isolation of DNA and MagnifiQ™ 16 Plant DNA instant kit (A&A Biotechnology, Gdańsk, Poland). The DNA concentration was measured with the SmartSpec PlusTM spectrophotometer. PCR was performed using the BioRad C1000 Touch thermal cycler with a heated cover (Bio-Rad, Hercules, CA, USA) in the 25-µL reaction solution (PCR Master MixPlus, A&A Biotechnology, Gdańsk, Poland) as described in detail in our

previous paper.[23] The PCR products were visualized on a UV transilluminator (GelDoc XR+ Gel Photodocumentation System with Image Lab 4.1 software, Bio-Rad, Hercules, CA, USA) after staining with SimplySafe™ (EURx, Sp. z o.o., Gdańsk, Poland). As a size reference, the Gene Ruler^{TM} Express DNA Ladder (Thermo Fisher Scientific, Waltham, MA, USA) was used. The banding patterns were recorded as binary matrices, where "1/0" indicates the presence/absence, respectively, of a given fragment. The numbers of monomorphic, polymorphic, and specific loci were counted.

Statistical Analysis

The experiment was set up in a completely randomized design. One-way analysis of variance (ANOVA) and post hoc Fisher's least significant difference (LSD) test ($p \leq 0.05$) were performed using Statistica 13.3 software (StatSoft Polska, Cracow, Poland) to determine the effects of nanoparticles treatment on the variability of analyzed traits. To identify the relationship between the distinguishing qualitative features under study, Spearman's rank correlation coefficients were determined at $p \leq 0.05$. The mean values and standard deviations (SD) were calculated. For data expressed as a percentage, before ANOVA analysis, the Freeman–Tukey double-arcsine transformation was performed. GenAlex 6.5 software[64] was used to run the principal component analysis (PCoA). Population groups were distinguished based on the analysis of molecular variance (AMOVA) estimates. Heterozygosity index (H), polymorphic information content (PIC), effective multiplex ratio (E), discriminating power (D), and resolving power (R) were investigated for every primer and marker system used.[65]

Results

In vitro Plant Regeneration in Response to NP-Treatment

Internodes treated with the tested nanoparticles presented a varied ability to regenerate adventitious shoots (Figures 2 and 3). The application of Co_3O_4 NPs resulted in the lowest share of regenerating explants (46.67%), in contrast to other experimental objects, where the values of this parameter ranged from 70% to 80.35%. Statistically, the control and Fe_3O_4@Co NP-treated internodes regenerated most shoots (3.59 and 4.22, respectively), whereas the use of CdS NPs (2.6) and, in particular, Co_3O_4 NPs (2.22), resulted in a strong limitation of shoot formation.

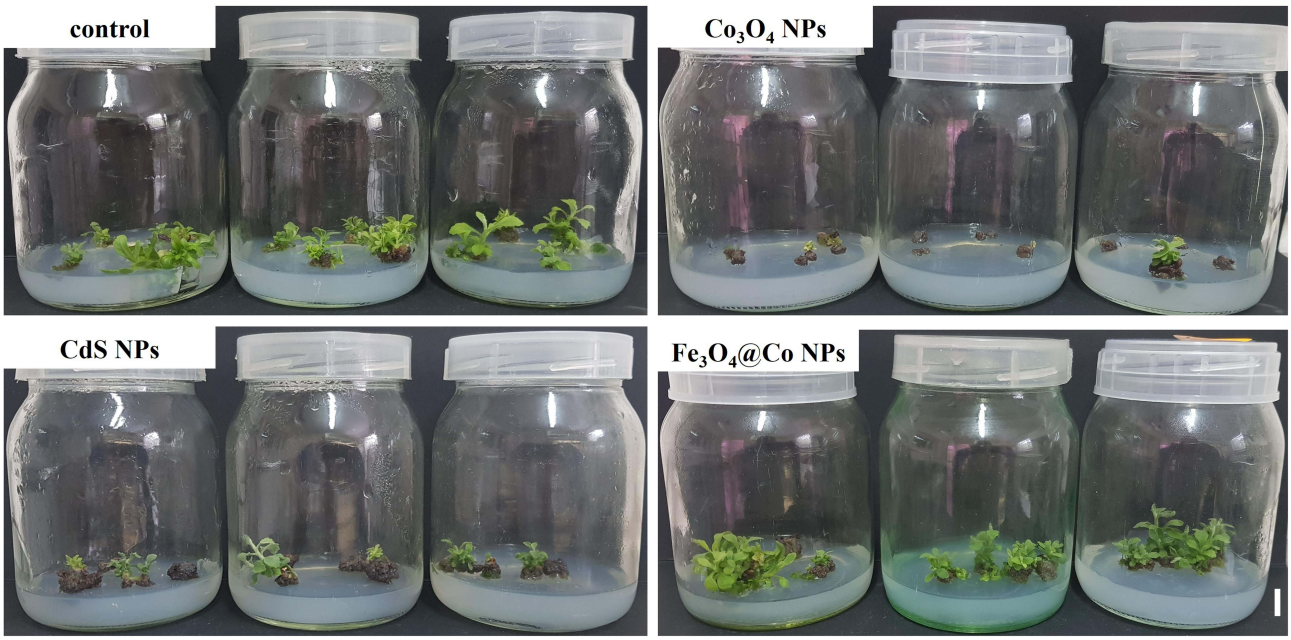

Figure 2 Adventitious shoots regeneration on *C. morifolium* 'Lilac Wonder' internodes after treatment with various types of nanoparticles, the eighth week of culture; bar = 1 cm.

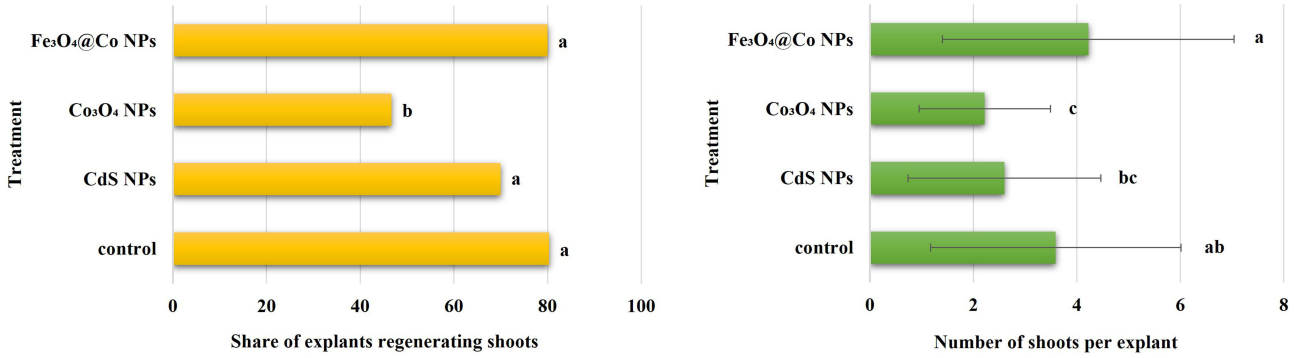

Figure 3 Efficiency of adventitious shoots regeneration on *C. morifolium* 'Lilac Wonder' internodes after treatment with various types of nanoparticles. Means or means ± Standard Deviation; (a–c) means on graphs followed by the same letter do not differ significantly at $p \leq 0.05$ (Fisher's test).

Plant Biochemical Activity in Response to NP-Treatment

In the tissues of shoots regenerated on internodes treated with the tested nanoparticles, a decrease in the relative flavonols content (0.050–0.053), and an increase in the anthocyanins content (0.042–0.046) was reported (Table 1). The content of flavonols and anthocyanins in the control was 0.062 and 0.033, respectively (Table 1). The shoots treated with CdS NPs had the lowest chlorophyll content (9.93), followed by those treated with Co_3O_4 NPs (10.28), while shoots treated with Fe_3O_4@Co NPs (10.45) and the control (10.70) showed the highest values. No significant differences were noted in the SPAD leaf greenness index value between experimental objects (32.79–33.68).

The application of Co_3O_4 NPs and Fe_3O_4@Co NPs resulted in a significant decrease of the value of minimal fluorescence (F_0) compared to the control (Table 2). Moreover, shoots treated with Co_3O_4 NPs were characterized by the lowest value of variable (F_V) and maximal (F_M) chlorophyll fluorescence. The control and CdS NP-treated shoots had the lowest F_V/F_M and F_V/F_0 ratios, followed by Co_3O_4 NP-treated shoots, while the Fe_3O_4@Co NP-treated shoots had the highest values of these parameters.

A significant effect of the tested nanoparticles on the stimulation of polyphenols biosynthesis was demonstrated (Table 3). The TCP was the highest in CdS NP- and Co_3O_4 NP-treated shoots (46.63 and 47.82 $mg \cdot g^{-1}$ DW, respectively). The content of polyphenols in Fe_3O_4@Co NP-treated shoots (43.04 $mg \cdot g^{-1}$ DW) was also statistically higher than in control shoots (38.74 $mg \cdot g^{-1}$ DW). As for the antioxidant capacity assay, the FRAP/ABTS values were significantly increased/decreased after NP applications, respectively, particularly for Co_3O_4 NP and Fe_3O_4@Co NP treatments.

Statistical analysis also showed a significant, more than two- to four-fold increase in the APOX and GPOX activity in shoots regenerated on the CdS NP-treated internodes compared to the other experimental objects, which did not differ in

Table 1 Relative Content of Flavonols, Anthocyanins, Chlorophyll, and SPAD Index in *C. morifolium* 'Lilac Wonder' Adventitious Shoots After Treatment with Various Types of Nanoparticles

Treatment	Flavonols	Anthocyanins	Chlorophyll	SPAD Index
Control	0.062±0.028[a]	0.033±0.010[c]	10.70±1.98[a]	33.68±4.51[a]
CdS NPs	0.050±0.029[b]	0.046±0.010[a]	9.93±1.32[b]	32.79±2.13[a]
Co_3O_4 NPs	0.053±0.025[b]	0.043±0.009[ab]	10.28±1.53[ab]	33.30±2.49[a]
Fe_3O_4@Co NPs	0.050±0.024[b]	0.042±0.009[b]	10.45±1.29[a]	33.63±1.99[a]

Notes: Means ± Standard Deviation; [a,b,c]Means in columns followed by the same letter do not differ significantly at $p \leq 0.05$ (Fisher's test).
Abbreviation: SPAD index, Soil Plant Analysis Development index.

https://doi.org/10.2147/NSA.S557241

Table 2 Chlorophyll Fluorescence Indices in *C. morifolium* 'Lilac Wonder' Adventitious Shoots After Treatment with Various Types of Nanoparticles

Treatment	F_0	F_V	F_M	F_V/F_M	F_V/F_0
Control	177.42±6.23[a]	787.70± 18.87[ab]	965.13±19.72[a]	0.816±0.006[b]	4.44±0.19[b]
CdS NPs	176.30±5.47[ab]	785.95±18.82[ab]	962.25±20.09[ab]	0.816±0.006[b]	4.46±0.17[b]
Co_3O_4 NPs	174.50±5.66[b]	780.55±26.08[b]	955.05±29.74[b]	0.817±0.004[ab]	4.47±0.13[ab]
Fe_3O_4@Co NPs	174.88±5.12[b]	792.90±13.89[a]	967.78±17.35[a]	0.819±0.004[a]	4.54±0.11[a]

Notes: Means ± Standard Deviation; [ab]Means in columns followed by the same letter do not differ significantly at $p \leq 0.05$ (Fisher's test).
Abbreviations: F_0, minimal fluorescence; F_v, variable fluorescence; F_M, maximal fluorescence.

Table 3 TCP, FRAP, and ABTS Analysis in *C. morifolium* 'Lilac Wonder' Adventitious Shoots After Treatment with Various Types of Nanoparticles

Treatment	TCP (mg g^{-1} DW)	FRAP (mg TEAC g^{-1} DW)	ABTS (mg mL^{-1})
Control	38.74±1.91[c]	358.80±4.35[c]	1.08±0.01[a]
CdS NPs	46.63±1.16[a]	443.00±2.94[b]	1.06±0.02[b]
Co_3O_4 NPs	47.82±0.82[a]	629.80±9.13[a]	0.61±0.02[d]
Fe_3O_4@Co NPs	43.04±0.58[b]	610.20±4.35[a]	0.80±0.01[c]

Notes: Means ± SD; [abc]Means in columns followed by the same letter do not differ significantly at $p \leq 0.05$ (Fisher's test). Spearman's rank correlation: ABTS/TCP: r = 0.61, FRAP/TCP: r = 0.75; at $p \leq 0.05$.
Abbreviations: TCP, total content of polyphenols; FRAP, ferric reducing antioxidant power; ABTS, [2,2'-azino-bis (3-ethylbenzothiazoline-6-sulfonic acid)] assay; DW, dry weight.

this respect (Table 4). Interestingly, the SOD activity was the lowest in control shoots (14.89 U), and significantly higher in most NPs-treated shoots (18.09–18.36 U), except for Co_3O_4 NPs (17.67 U).

Plant Phenotype Variability in Response to NP-Treatment

During glasshouse cultivation, the share of flowering plants varied depending on the experimental treatment (Table 5, Figure 4A and B). A vast majority of standard (90%) and control plants (83.33%) formed inflorescences. As for CdS NPs and Co_3O_4 NPs treatments, the share of flowering plants was lower, and amounted to 73.15% and 76.84%, respectively. Phenotypic evaluation of inflorescences did not show qualitative variability of ligulate florets' color. The inflorescences were pink; however, quantitative changes related to the different content of anthocyanins and color intensity appeared.

Table 4 APOX, GPOX, and SOD Activity (U) in *C. morifolium* 'Lilac Wonder' Adventitious Shoots After Treatment with Various Types of Nanoparticles

Treatment	APOX	GPOX	SOD
Control	32.08±11.07[b]	8.38±4.46[b]	14.89±4.56[b]
CdS NPs	137.42±82.03[a]	36.51±16.26[a]	18.36±0.74[a]
Co_3O_4 NPs	32.14±14.78[b]	14.77±5.37[b]	17.67±2.19[ab]
Fe_3O_4@Co NPs	64.14±37.34[b]	12.43±3.91[b]	18.09±1.34[a]

Notes: Means ± Standard Deviation; [ab]Means in columns followed by the same letter do not differ significantly at $p \leq 0.05$ (Fisher's test).
Abbreviations: APOX, ascorbate peroxidase; GPOX, guaiacol peroxidase; SOD, superoxide dismutase.

Table 5 Flowering and Inflorescence Characteristics of *C. morifolium* 'Lilac Wonder' Plants During Glasshouse Cultivation: Standard, Control, and Adventitious Shoots After Treatment with Various Types of Nanoparticles

Treatment	No. of Acclimatized and ex vitro Cultivated Plants	No. (%) of Flowering Plants	Inflorescence Color and RHSCC Color Code	Content of Anthocyanins in Inflorescence (mg g^{-1} FW)
Standard	20	18 (90.00[a])	Light pink (63C/62D*)	0.456±0.055[c]
Control	78	65 (83.33[a])	Pink (70C/69A)	0.535±0.089[ab]
CdS NPs	108	79 (73.15[b])	Pink (70D/69A)	0.518±0.058[abc]
Co_3O_4 NPs	95	73 (76.84[b])	Light pink (65A/62D)	0.490±0.079[bc]
Fe_3O_4@Co NPs	115	94 (81.74[ab])	Pink (70C/69A)	0.588±0.035[a]

Notes: Means ± Standard Deviation; [abc]Means in columns followed by the same letter do not differ significantly at $p \leq 0.05$ (Fisher's test). Standard — plants propagated by the single-node method on the NP-free medium. Control — adventitious shoots regenerated on the NP-free medium. * inner/outer side of ligulate flower.
Abbreviations: RHSCC, The Royal Horticultural Society Colour Chart; FW, fresh weight.

The highest content of these pigments was found in ligulate flowers of plants treated with Fe_3O_4@Co NPs, and the lowest in the standard plants.

One individual (mutant) was phenotypically identified within Co_3O_4 NP-treated plants (Figure 4C and D). This plant developed leaves with variegation, ie, mosaic yellow-green discolorations on the leaf blades.

At the greenhouse cultivation stage, plants treated with Fe_3O_4@Co NPs (71.79 cm) and controls (69.28 cm) formed the longest stems. However, the stem length of plants treated with CdS NPs, and Co_3O_4 NPs did not differ statistically from the standard or control plants (Table 6). The Co_3O_4 NP-treated chrysanthemum developed more leaves (38.47) than standard plants (35.67). Control and NP-treated plants had a similar number of leaves. Leaf area of control and NP-treated plants (25.81–29.46 cm^2), except for Co_3O_4 NPs (30.80 cm^2), was lower than in the standard plants (33.95 cm^2).

Figure 4 Plants of *C. morifolium* 'Lilac Wonder' during the vegetative growth stage (**A**); plants at full flowering (**B**); variegated mutant found among Co_3O_4 NP-treated plants (**C**); leaf sample scan of the variegated mutant (**D**).

https://doi.org/10.2147/NSA.S557241

Table 6 Biometric Parameters of *C. morifolium* 'Lilac Wonder' Plants During Glasshouse Cultivation: Standard, Control, and Adventitious Shoots After Treatment with Various Types of Nanoparticles

Treatment	Stem Length (cm)	Number of Leaves	Leaf Area (cm^2)	Leaf Perimeter (cm)	Leaf Length (L) (cm)	Leaf Width (W) (cm)	Leaf Aspect Ratio (W/L)
Standard	66.08±5.85^{b}	35.67±2.16^{b}	33.95±10.81^{a}	43.39±10.15^{a}	10.46±1.76^{a}	6.62±0.93^{a}	0.64±0.05^{a}
Control	69.28±5.16^{ab}	37.00±1.97^{ab}	29.46±8.31^{bc}	41.74±7.94^{a}	10.10±1.50^{a}	6.09±0.77^{b}	0.61±0.06^{ab}
CdS NPs	67.05±5.20^{b}	37.80±2.78^{ab}	25.81±6.56^{c}	37.58±5.49^{b}	9.25±1.27^{b}	5.62±0.82^{c}	0.61±0.07^{ab}
Co_3O_4 NPs	66.95±5.82^{b}	38.47±3.12^{a}	30.80±9.99^{ab}	42.32±6.22^{a}	10.36±1.65^{a}	6.16±0.94^{b}	0.60±0.06^{bc}
Fe_3O_4@Co NPs	71.79±3.40^{a}	38.42±3.95^{ab}	29.36±5.89^{bc}	42.13±6.40^{a}	10.36±1.20^{a}	5.94±0.65^{bc}	0.58±0.05^{c}

Notes: Means ± Standard Deviation; ^{abc}Means in columns followed by the same letter do not differ significantly at $p \leq 0.05$ (Fisher's test). Standard — plants propagated by the single-node method on the NP-free medium. Control — adventitious shoots regenerated on the NP-free medium.

Leaves of CdS NP-treated plants had the lowest perimeter, length, and width. The highest (0.64) and the lowest (0.58) leaf aspect ratios were found in the standard and Fe_3O_4@Co NP-treated plants, respectively.

Plant Genotype Variability in Response to NP-Treatment

A total of 3707 and 6202 scorable bands were detected by eight RAPD and eight SCoT primers in 86 chrysanthemum plants, respectively (Table 7). Among the molecular marker systems tested, SCoTs generated more products and polymorphisms. Primer S-4 generated the highest number of bands (16 per sample), while primer S-2 produced seven amplicons per sample. Four primers detected 11 polymorphic loci (including five specific) in a total of six specimens (ie, 7.0% of all plants analyzed). The highest number of polymorphic plants (4) was obtained with the S-6 primer. As for the RAPD analysis, three primers detected three polymorphic and five specific bands in seven samples (8.1% of all analyzed plants). Primer R-4 generated the highest number of bands in this marker system (12 per sample), but R-2 was most effective in screening for variation. In contrast, primers R-5 and R-6 generated only one product (Table 7).

Table 7 Comparative Analysis of Molecular Products Obtained From *C. morifolium* 'Lilac Wonder' Plants Analyzed with RAPD and SCoT Marker Systems

Primer Code	Primer Sequence 5' → 3'	Total no. of Bands	No. of loci				No. and (%) of Plants with Polymorphism	No. of Genotypes
			Total	Mono.	Poly.	Spec.		
		RAPD						
R-1	GGG AAT TCG G	516	6	6	0	0	0	1
R-2	GAC CGC TTG T	350	5	4	1	0	6 (7.0)	2
R-3	GGA CTG GAG T	604	9	7	0	2	1 (1.2)	2
R-4	GCT GCC TCA GC	775	12	7	2	3	1 (1.2)	2
R-5	TAC CCA GGA GCG	86	1	1	0	0	0	1
R-6	CAA TCG CCG T	86	1	1	0	0	0	1
R-7	GGT GAC GCA G	774	9	9	0	0	0	1
R-8	CCC AGT CAC T	516	6	6	0	0	0	1
∑ (mean)		3707 (463.373)	49 (6.125)	41 (5.125)	3 (0.375)	5 (0.625)	7 (8.1) -	3 -

(*Continued*)

Table 7 (Continued).

Primer Code	Primer Sequence 5' → 3'	Total no. of Bands	No. of loci				No. and (%) of Plants with Polymorphism	No. of Genotypes
			Total	Mono.	Poly.	Spec.		
		SCoT						
S-1	CAA CAA TGG CTA CCA CCG	688	8	0	0	0	0	1
S-2	CAA CAA TGG CTA CCA CCT	602	7	0	0	0	0	1
S-3	CAA CAA TGG CTA CCA CGT	604	8	7	1	0	2 (2.3)	2
S-4	ACG ACA TGG CGA CCA ACG	1205	16	13	1	2	1 (1.2)	2
S-5	ACC ATG GCT ACC ACC GTC	605	11	5	3	3	3 (3.5)	4
S-6	ACC ATG GCT ACC ACC GTG	692	9	8	1	0	4 (4.7)	2
S-7	CCA TGG CTA CCA CCG CCA	688	8	0	0	0	0	1
S-8	CCA TGG CTA CCA CCG CAG	1118	13	0	0	0	0	1
∑ **(mean)**		6202 (775.25)	81 (10.125)	33 (4.125)	6 (0.75)	5 (0.625)	6 (7.0) -	6 -

Abbreviations: RAPD, Randomly Amplified Polymorphic DNA; SCoT, Start Codon Target Polymorphism; mono., monomorphic; poly., polymorphic; spec., specific (present in a single band profile).

Among the two marker systems used, higher mean H, PIC, E, D, and R values were reported with SCoTs (Table 8). When comparing individual primers, S-5 generated the highest heterozygosity index, discriminating power, and resolving power, while S-4 had the highest effective multiplex ratio. For PIC, R-2 was notable among RAPD primers (Table 8).

Table 8 Values of Heterozygosity Index (H), Polymorphic Information Content (PIC), Effective Multiplex Ratio (E), Marker Index (MI), Discriminating Power (D), and Resolving Power (R) of the Marker Systems Used in the Study

Primer	H	PIC	E	D	R
	RAPD				
R-1	0.000	0.000	0.000	0.000	0.000
R-2	0.303	0.305	4.070	0.338	0.140
R-3	0.343	0.292	7.023	0.391	0.047
R-4	0.374	0.281	9.012	0.436	0.116
R-5	0.000	0.000	0.000	0.000	0.000
R-6	0.000	0.000	0.000	0.000	0.000
R-7	0.000	0.000	0.000	0.000	0.000
R-8	0.000	0.000	0.000	0.000	0.000
Mean	0.128	0.110	2.513	0.146	0.038

(*Continued*)

https://doi.org/10.2147/NSA.S557241

Table 8 (Continued).

Primer	H	PIC	E	D	R
	SCoT				
S-1	0.000	0.000	0.000	0.000	0.000
S-2	0.000	0.000	0.000	0.000	0.000
S-3	0.214	0.271	7.023	0.229	0.047
S-4	0.218	0.270	14.012	0.233	0.070
S-5	0.461	0.188	7.035	0.591	0.163
S-6	0.189	0.276	8.047	0.201	0.093
−7	0.000	0.000	0.000	0.000	0.000
S-8	0.000	0.000	0.000	0.000	0.000
Mean	0.135	0.126	4.515	0.157	0.047

Abbreviations: RAPD, Randomly Amplified Polymorphic DNA; SCoT, Start Codon Target Polymorphism.

According to the PCoA analysis based on RAPD genotyping, three agglomerations could be distinguished (Figure 5). The largest group comprised 61 homogenous, monomorphic plants with no variation detected compared with the non-treated adventitious control or meristematic-derived standard. Polymorphic specimens were placed in two groups. The first included four plants treated with CdS NPs, one treated with Fe_3O_4@Co NPs, and one control. These plants had the same genotype. The population most distant from the predominant control and standard consisted of a single specimen treated with CdS NPs.

As for the PCoA analysis based on the SCoT marker system, the plants studied were grouped into four agglomerations. Due to the minor genetic variation detected in two specimens treated with Co_3O_4 NPs, these plants were placed in a single agglomeration with the control and other monomorphic plants (Figure 5). Three plants obtained from the Fe_3O_4 @Co treatment were grouped into two distinct populations. The most altered genotype, treated with CdS NPs, was included in a separate group. This was the only plant considered polymorphic by both marker systems used. The remaining polymorphic genotypes did not overlap in the RAPD and SCoT analyses.

Following the AMOVA analysis, most of the genetic variation detected by the RAPD and SCoT markers in chrysanthemum 'Lilac Wonder' was considered intra-population origin. Nevertheless, 2–3% of the variation was caused by nanoparticles. Example band profiles are shown in Figure 6.

Discussion

In the present study, the use of 75 $mg \cdot L^{-1}$ CdS NPs and Co_3O_4 NPs reduced the efficiency of adventitious shoot regeneration compared to the control internodes. However, a statistically similar number of shoots was regenerated on the Fe_3O_4@Co NP-treated and control explants. In our previous experiments, the application of Ag NPs at concentrations of 20–100 $mg \cdot L^{-1}$ also strongly limited the formation of adventitious shoots on internodes and leaf explants in *C. morifolium*, resembling the action of physical or chemical mutagens.[20,21] It is well known that nanoparticles alter biological architecture in many complex and not fully understood ways.[4] Nanoparticles can lead to changes at the molecular level and consequently affect the overall plant physiology, growth, and development, including shoot and root formation.[7] It is assumed that each type of nanoparticles imparts distinct effects on physiological processes via different signaling cascades. Possible pathways through which nanoparticles influence plant regeneration include modulation of hormonal levels, increased ROS production, and potential epigenetic modifications. Nanoparticles have been found to cause lipid membrane peroxidation in plant cells, leading to loss of membrane integrity, ultimately hampering the

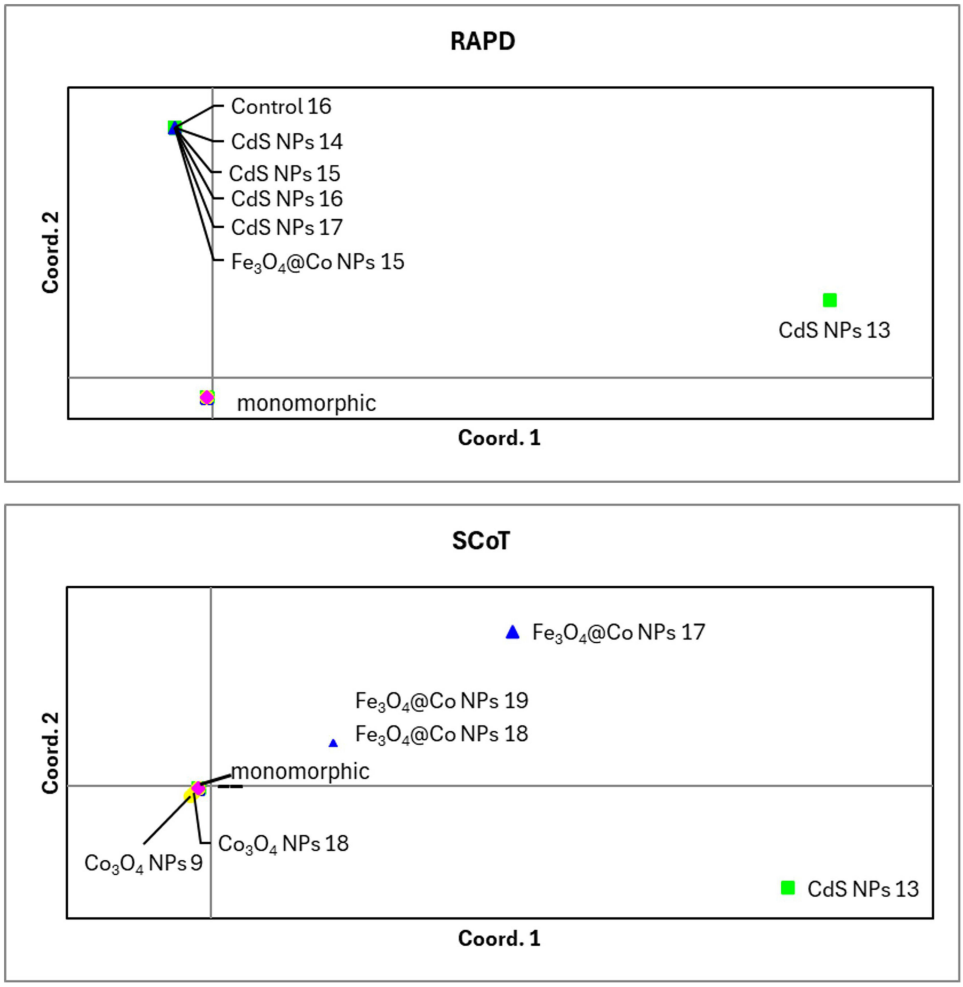

Figure 5 Graphs of principal coordinates analysis (PCoA) of *C. morifolium* 'Lilac Wonder' individuals after treatment with various types of nanoparticles; based on Randomly Amplified Polymorphic DNA (RAPD) and Start Codon Target Polymorphism (Scot) markers.

regeneration potential. They can also reduce cell survival by altering the expression of nucleic acids, causing DNA damage, disrupting chlorophyll synthesis, and causing electrolyte leakage.[1] Nanoparticles can cause phytotoxicity and negatively affect the overall metabolism of plants, but at the same time, their unique properties can also be used to improve plant functioning.[8] The key factors determining the stimulation or inhibition of in vitro regeneration by nanoparticles seem to be their chemical composition, the concentration at which they are applied to the plants, and the plant genotype itself.

One of the main harmful effects of nanoparticles on plant cells is the induction of oxidative stress, which is a complex physiological, biochemical, and molecular phenomenon resulting from the overproduction and accumulation of ROS.[8] Reactive oxygen species can cause serious damage to cellular components, including proteins, lipids, carbohydrates, and DNA. Although plants have innate antioxidant defense mechanisms to mitigate the effects of ROS, these mechanisms often fail, leading to oxidative damage, stunted growth, and reduced productivity.[66] Stress conditions can reduce the content of chlorophyll, leading to reduced plant growth and development.[11] Polyphenols, including flavonols, are non-enzymatic antioxidant molecules produced by plants mainly to mitigate stress and participate in detoxification reactions, acting as metal chelators in the scavenging of ROS by peroxidases.[67,68] SOD, APOX, and GPOX belong to the group of enzymatic antioxidants that catalyze the degradation of ROS. Changes in the content of non-enzymatic antioxidants and the activity of the above-mentioned enzymes are biological markers of oxidative stress.[51] Results of the present study revealed that the tested nanoparticles also influenced the biochemical activity of regenerated plants. The tissues of NP-treated shoots accumulated less flavonols, but more total polyphenols and anthocyanins, and showed increased

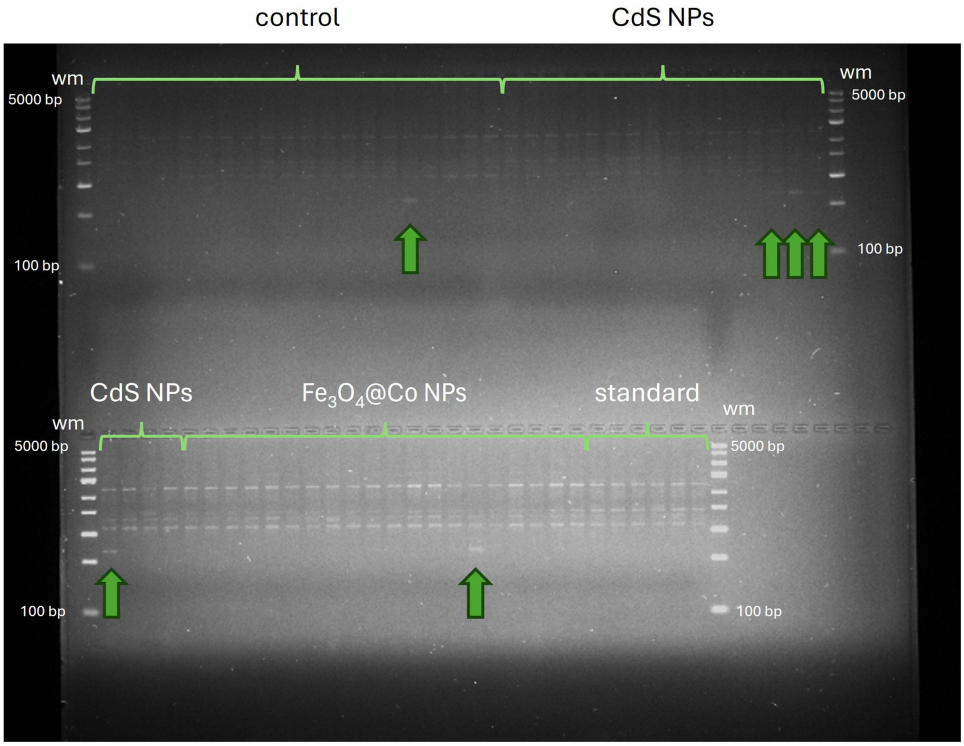

Figure 6 Example Randomly Amplified Polymorphic DNA (RAPD) band profiles of *C. morifolium* 'Lilac Wonder' received as a result of nanoparticles treatment (primer R-2). Outermost lanes are DNA base pair weight markers (wm), while inner lines represent control plants, plants treated with nanoparticles, and the standard. Arrows point to polymorphic genotypes.

antioxidant activity compared to the control shoots. The highest activity of oxidative stress enzymes (APOX, GPOX, and SOD), and at the same time, the lowest chlorophyll content were noted in the shoots treated with CdS NPs. Similarly, tomato (*Solanum lycopersicum* L.) plants treated with multiwalled carbon nanotubes produced less flavonoids and more anthocyanins.[69] Manganese nanoparticles (Mn NPs) used at the concentrations of 125 and 250 mg·mL^{-1} also increased the activity of SOD and peroxidases (POX), and reduced the chlorophyll content in wheat (*Triticum aestivum* L.), which indicated the occurrence of stress.[70]

There are many different methods for determining antioxidant activity.[71,72] In the present study, two methods with varying mechanisms of action were used. The ABTS test with 2,2'-azino-bis(3-ethylbenzothiazoline-6-sulfonic acid) is based on free radical scavenging, whereas the FRAP test is based on the reduction of the Fe^{3+}TPTZ salt to its blue form Fe^{2+}TPTZ.[72] The tested nanoparticles increased the antioxidant activity measured by the FRAP method, which confirmed the increase in the reducing capacity of the NP-treated plants. The strongest effect was obtained after the application of Co_3O_4 and Fe_3O_4@Co NPs, indicating their potential properties, which induce defense mechanisms in the plant. A similar effect was observed for the ABTS assay, where a loss of color and a decrease in absorbance could be explained by the interaction of antioxidants with ABTS radicals. The highest ABTS quenching activity was obtained for Co_3O_4 and Fe_3O_4@Co NPs. Other studies also indicate a significant effect of nanoparticles on the non-enzymatic antioxidant capacity of plants.[73,74] Wei et al[74] observed an increase in the FRAP parameter in *S. lycopersicum* plants cultivated in soil with SiO_2 NPs. Likewise, Thakur et al[73] observed the FRAP increase in wheat (*Triticum aestivum* L.) seedlings after the application of ZnO and TiO_2 NPs at two concentrations (1.5 mg·L^{-1} and 10 mg·L^{-1}). Owji et al[75] reported a decrease in the FRAP antioxidant potential of fenugreek (*Trigonella foenum-graceum* L.) treated with 100 µg·mL^{-1} Al_2O_3 NPs. The mechanism of nanoparticles' action on the non-enzymatic antioxidant potential of plants can be complex and depends on the type, concentration, and the method of application.[76–78] Nanoparticles can be applied to plants in various ways (eg, through roots, leaves, seeds) and, due to the ability to penetrate the cells, they interact with many cellular structures.[79,80] These interactions can initiate several physiological responses, eg, increased production of

ROS or modulation of metabolic pathways. Probably, one of the main nanoparticles effects is the modification of the phenylpropanoid pathway, in which phenolic compounds with antioxidant properties are synthesized.[81] However, the action of nanoparticles is biphasic. In appropriate concentrations, they can act as a mild stress factor („priming"), activating plant defense mechanisms, and in excessive concentrations, they can cause oxidative stress, leading to lipid peroxidation, membrane and DNA damage, and exceeding compensatory capacities, which can lead to the inhibition of secondary metabolism and reduced antioxidant potential.[82] Our results also indicated a high correlation between the content of polyphenols and the antioxidant potential of the tested samples (ABTS/TCP: r = 0.61, FRAP/TCP: r = 0.75). Similarly, Patil et al[83] analyzed the antioxidant potential of 22 chrysanthemum cultivars. They obtained a correlation at the level of r = 0.40, while Cao et al[84] observed r = 0.64 in studies with five chrysanthemum cultivars.

In the present study, the nanoparticles treatment also had a subsequent effect on the further ex vitro growth and development of chrysanthemum shoots, and may be important as a factor modifying the growth force and habit of plants. Chrysanthemums treated with Fe_3O_4@Co NPs formed the longest shoots, whereas the application of CdS NPs and Co_3O_4 NPs had the opposite effect. In addition, shoots regenerated in the presence of CdS NPs developed the smallest leaves. This effect can be correlated with the sulphur bioavailability and toxicity. The observed effects are also consistent with the biometric results obtained for maize treated with CdS NPs[25] or for chrysanthemum treated with Fe_3O_4.[36] Iron oxide nanoparticles also promoted shoot elongation of chrysanthemum plants developed in vitro from synthetic seeds.[85] Iron is an essential micronutrient involved in many metabolic pathways (eg, DNA synthesis, respiration, and photosynthesis) in plants. It is a component of many vital enzymes, stimulates chloroplast synthesis, and is responsible for maintaining the structure and function of chloroplasts.[86] The physiological importance of iron could cause the observed stimulation of growth in contrast to cadmium, sulphur, and cobalt. However, this element can be potentially toxic and can promote ROS formation.[86] The effects of various mutagens, including radiation and nanoparticles, can cause varying effects in stimulating plant growth. Low doses can stimulate, while higher doses can limit shoot growth.[17,21,87]

Biochemical analysis of inflorescences revealed quantitative changes in anthocyanins content. The highest amounts of these pigments were found in ligulate flowers of Fe_3O_4@Co NP-treated plants, and the lowest in plants treated with Co_3O_4 NPs and in standard plants. Cobalt is known to influence several enzymes in plants, acting as a cofactor or signaling agent at low concentrations. Hence, the different anthocyanins accumulation can be closely correlated with the variation in Co dosage and bioavailability between the two NP-based formulations. Enhanced anthocyanin biosynthesis in Fe_3O_4@Co NP-treated chrysanthemums can be stimulated by low cobalt dosage, while Co_3O_4 NPs can deliver cobalt faster or in a less regulated manner. At the same time, the Fe ions availability in Fe_3O_4@Co NPs may reduce the oxidative stress and indirectly influence pigment accumulation, resulting in more intense inflorescence pigmentation. A decrease or increase in the content of anthocyanins, along with the associated change in the intensity of inflorescence color, is often observed in plants exposed to X or gamma irradiation, or Ag NPs, as reported in our previous studies on induced mutagenesis in chrysanthemum.[20,21,88] Qualitative changes resulting from the appearance or disappearance of carotenoid pigments are also very desirable and manifest themselves as a change in inflorescence color compared to the mother cultivar.[17,20,21] No such change was observed in the present study, suggesting that the tested nanoparticles do not have a high potential to induce phenotypically manifested mutations of inflorescence traits; however, one individual (mutant) identified among Co_3O_4 NP-treated plants had variegated leaves. Variegated plants usually have leaves with green and white (or yellow) sectors. Cells in the green sectors contain typical chloroplasts, whereas chloroplasts in the white (or yellow) sectors lack chlorophyll and/or carotenoid pigments and appear to be blocked at different stages of biogenesis. Variegations may be caused by nuclear, chloroplast, or mitochondrial gene mutations. Variegated sectors may have different genotypes (chimeras) or the same (mutant) genotype. In mutagenesis experiments, variegations arise at a low, but variable, frequency.[89,90] In our study, variegation occurred with a frequency of 1.05%. In studies with *Arabidopsis thaliana*, the frequency of variegation was 0.04–0.2% in genetic transformation experiments, and 10% in experiments with chemical and physical mutagens.[90] Bajpay and Dwivedi[87] obtained variegated chrysanthemums with a frequency of 10–22.66% after irradiation with gamma rays at very high doses of 100, 150, 200, and 250 Gy. Treatment with gamma rays was also a source of variegated chrysanthemum plants, with a frequency of 5%, in a breeding experiment performed by Mandal et al.[91] According to these authors, the novel chlorophyll variegated chrysanthemums

were attractive, and variegation gives additional beauty to the plant throughout the vegetative stage of growth. It can be concluded that the frequency of variegation is highly influenced by the type and dose of mutagen used.

The present study aimed to assess the applicability of nanoparticles as potential mutagens in chrysanthemum breeding by evaluating the genetic variation induced by different nanoparticle types using RAPD and SCoT markers. The results indicate that nanoparticles can induce genetic variation in chrysanthemum, although to a limited extent. SCoT markers generated more amplicons and polymorphisms compared to RAPDs, confirming previous findings that SCoTs are more efficient in detecting genetic variation in plants.[92,93] RAPD genotyping identified three polymorphic and five specific bands in seven samples, while SCoTs identified 11 polymorphic loci (including five specific) in six specimens, with only one specimen overlapping between the two marker systems. This indicates that various marker systems capture different aspects of the genetic changes induced by nanoparticles. The AMOVA results suggest that nanoparticles do contribute to mutation occurrence in chrysanthemum. This is consistent with studies showing that Ag NPs can induce genetic, biochemical, and phenotypic variation in chrysanthemum.[20] The present study, however, proves that different types of nanoparticles have divergent mutagenic potential. In the current analysis, only one specimen treated with CdS NPs was identified as polymorphic by both marker systems (five primers). This suggests that this particular nanoparticle type is more useful in breeding than Fe_3O_4@Co NPs or Co_3O_4 NPs. On the other hand, CdS NPs are still less effective than Ag NPs as the latter nanoparticles induced genetic variation that manifested in the form of a change in the inflorescence colour,[20,21] which was not reported in the present study. The varied effects of CdS, Co_3O_4, and Fe_3O_4@Co nanoparticles on mutation induction in chrysanthemum can be related to their differences in physicochemical properties (size, solubility, and surface chemistry), metal ion release, and redox activity that affect cellular uptake and bioavailability. CdS nanoparticles easily release Cd^{2+} ions, which are highly genotoxic and interact directly with DNA and proteins.[94] On the other hand, Co_3O_4, and Fe_3O_4@Co NPs act mostly as redox catalysts, generating ROS.[95] Das and Mohanty[96] evaluated the toxicological impacts of cadmium, cobalt, and copper in radish (*Raphanus sativus* L.), lettuce (*Lactuca sativa* L.), and wheat (*Triticum aestivum* L.). They found that Cd inhibited seed germination and seedling growth more potently than Co or Cu. Co was toxic at a higher concentration (50 μM), but Cd was even more deleterious at a lower (10 μM) dose. These findings corroborate our results and explain why only this particular treatment caused the most excessive mutation.

Traditional mutation breeding in chrysanthemum involves physical mutagens like ionizing radiation or chemical mutagens such as ethyl methanesulfonate (EMS).[17] These methods can induce significant changes in flower color, shape, and size.[97] Previous studies suggest that gamma and X-rays have a 5–30% or 3–20% mutation efficiency, respectively, depending on dose and cultivar.[19,98] According to some researchers, chemical mutagens are even more effective.[99] While nanoparticles offer a potentially easier method for inducing mutations, as they can be added directly to the culture medium without specialized equipment, the extent of genetic variation caused by nanoparticles in this study appears to be more limited compared to conventional techniques. Nonetheless, a yield of 7–8.1% mutated plants confirms their utility in breeding. Begum and Dasgupta[99] and Shahwar et al[100] reported that the lowest dose of γ-rays (200 Gy) and lower concentration of EMS (0.1%), caffeine (0.1%), $Pb(NO_3)_2$ (20 $mg \cdot L^{-1}$), and $Cd(NO_3)_2$ (20 $mg \cdot L^{-1}$) showed the highest mutagenic efficiency in all genotypes studied. Perhaps also in chrysanthemum, modifying the concentration of nanoparticles could improve the results.

In summary, the present study suggests that although nanoparticles can induce biochemical, genetic, and phenotypic changes, careful selection of marker systems and screening methods is crucial for this variation identification. Further research is needed to optimize nanoparticle treatments and explore their potential in combination with other breeding techniques to increase genetic diversity and create new chrysanthemum cultivars.

Conclusion

Our results contribute to a better understanding of the multifaceted effects of various nanoparticles on plants in vitro and ex vitro at the biochemical, genetic, and phenotypic levels. They are of scientific and practical importance for the development of modern horticulture. We elaborated an innovative approach in plant breeding, proposing the use of nanoparticles as a source of variability induction. Ease of use and lower toxicity compared to conventional mutagens make nanoparticles a valuable addition to breeding methods for the semiconducting properties of the demonstrated particles, which, besides

indirect oxidative stress generation by the disruption of metabolic and/or electron transfer processes, can catalyze ROS, directly affecting the plant. The results are certainly interesting for scientists and chrysanthemum breeders.

The use of CdS NPs and Co_3O_4 NPs limited the efficiency of chrysanthemum adventitious organogenesis. Nanoparticles also modulated the biochemical activity of regenerating shoots. The induction of oxidative stress was most evident for CdS NPs application. Nanoparticles also affected the ex-vitro growth of chrysanthemums by modifying the habit of plants and leaf architecture. One mutant with variegated leaves was phenotypically identified within Co_3O_4 NP-treated plants. The use of nanoparticles also induced genetic variation, with CdS NPs causing the most distinct polymorphic changes, as confirmed by both RAPD and SCoT markers. While Fe_3O_4 @Co NPs and Co_3O_4 NPs also generated polymorphic genotypes, their effects were less evident, suggesting that nanoparticles vary in mutagenic potential, but could serve as a novel tool for plant breeding. The proposed use of nanoparticles for variability induction is also an innovative approach in plant biotechnology.

The plant in vitro culture system has tremendous potential in breeding, which is still not fully exploited. The addition of nanoparticles to the culture medium can be a relatively cost-effective, easy, and effective way to induce variation for breeding. To improve the frequency of observed mutations in future studies, it is recommended to use the tested nanoparticles in even higher concentrations, especially 100, 150, and 200 $mg \cdot L^{-1}$, as well as to focus the research on testing other types of nanoparticles containing cobalt and cadmium. The genotoxic effect of nanoparticles should also be experimentally tested in other plant genotypes.

Data Sharing Statement

Data available by Email on reasonable request.

Ethics Statement

We declare that no additional approvals were required in our study to conduct experiments with plant material, in accordance with institutional/local regulations. We also do not have queries regarding the ethical requirements.

Funding

Financially supported by the Minister of Science under the program “Regional Initiative of Excellence” (RID/SP/0017/2024/01).

Disclosure

The authors report no conflicts of interest in this work.

References

1. Guha PS, Gupta SD, Saha N. Nano-gardening: harnessing metal nanoparticles for enhanced in vitro plant regeneration. *BioNanoScience*. 2024;14(3):3555–3571. doi:10.1007/s12668-024-01548-0
2. Aslam F, Minhas LA, Kaleem M, et al. Sustainable synthesis of cobalt oxide nanoparticles (Co_3O_4-NPs) using extract of *Nodosilinea nodulosa*: characterization and potential biological applications. *BioNanoSci*. 2024;14:4764–4778. doi:10.1007/s12668-024-01551-5
3. Zeng Z, Wang Y, Wang H, et al. Nanomaterials: cross-disciplinary applications in ornamental plants. *Nanotechnol Rev*. 2024;13(1):20240049. doi:10.1515/ntrev-2024-0049
4. Zhou X, El-Sappah AH, Khaskhoussi A, et al. Nanoparticles: a promising tool against environmental stress in plants. *Front Plant Sci*. 2025;15:1509047. doi:10.3389/fpls.2024.1509047
5. Pacheco I, Buzea C. Nanoparticle interactions with plants. In: Ghorbanpour M, Manika K, Varma A editors. *Nanoscience and Plant-Soil Systems*. Springer International Publishing Ag; 2017:323–355. doi:10.1007/978-3-319-46835-8_12
6. Yan A, Chen Z. Impacts of silver nanoparticles on plants: a focus on the phytotoxicity and underlying mechanism. *IJMS*. 2019;20(5):1003.
7. Mittal D, Kaur G, Singh P, et al. Nanoparticles-based sustainable agriculture and food science: recent advances and future outlook. *Front Nanotechnol*. 2020;2:2020. doi:10.3389/fnano.2020.579954
8. Kumar V, Sharma M, Khare T, et al. Chapter 17 - Impact of nanoparticles on oxidative stress and responsive antioxidative defense in plants. In: Tripathi DL, Ahmad P, Sharma S, Kumar Chauhan D, Dubey NK, editors. *Nanomaterials in Plants, Algae, and Microorganisms*. Academic Press; 2018:393–406. doi:10.1016/B978-0-12-811487-2.00017-7
9. Álvarez SP, Tapia MAM, Vega MEG, et al. Nanotechnology and plant tissue culture. In: Prasad R, editor. *Plant Nanobionics. Nanotechnology in the Life Sciences*. Cham: Springer; 2019:333–370. doi:10.1007/978-3-030-12496-0_12
10. Horie M, Tabei Y. Role of oxidative stress in nanoparticles toxicity. *Free Radic Res*. 2020;55(4):331–342. doi:10.1080/10715762.2020.1859108

11. Khan I, Awan SA, Raza MA, et al. Silver nanoparticles improved plant growth and reduced the sodium and chlorine accumulation in pearl millet: a life cycle study. *Environ Sci Pollut Res*. 2021;28:13712–13724. doi:10.1007/s11356-020-11612-3
12. Sharma P. Chapter 6 - Genotoxicity of the nanoparticles. In: Chauhan NS, Gill SS editors. *Nanomaterial-Plant Interactions, the Impact of Nanoparticles on Agriculture and Soil*. Academic Press; 2023:115–128. doi:10.1016/B978-0-323-91703-2.00017-8
13. Gowtham HG, Shilpa N, Brijesh Singh S, et al. Toxicological effects of nanoparticles in plants: mechanisms involved at morphological, physiological, biochemical and molecular levels. *Plant Physiol Bioch*. 2024;210:108604. doi:10.1016/j.plaphy.2024.108604
14. Abdelsalam NR, Abdel-Megeed A, Ali HM, et al. Genotoxicity effects of silver nanoparticles on wheat (*Triticum aestivum* L.) root tip cells. *Ecotoxicol Environ Saf*. 2018;155:76–85. doi:10.1016/j.ecoenv.2018.02.069
15. Marmiroli M, Marmiroli N, Pagano L. Nanomaterials induced genotoxicity in plant: methods and strategies. *Nanomaterials*. 2022;12(10):1658. doi:10.3390/nano12101658
16. Park CH, Chae SC, Park S-Y, et al. Anthocyanin and carotenoid contents in different cultivars of chrysanthemum (*Dendranthema grandiflorum* Ramat.) flower. *Molecules*. 2015;20(6):11090–11102. doi:10.3390/molecules200611090
17. Miler N, Jedrzejczyk I, Jakubowski S, et al. Ovaries of chrysanthemum irradiated with high-energy photons and high-energy electrons can regenerate plants with novel traits. *Agronomy*. 2021;11(6):1111. doi:10.3390/agronomy11061111
18. Gu J, Scotti F, Reich E, et al. Chrysanthemum species used as food and medicine: understanding quality differences on the global market. *S Afr J Bot*. 2022;148:123–134. doi:10.1016/j.sajb.2022.04.009
19. Su J, Jiang J, Zhang F, et al. Current achivements and future prospects in the genetic breeding of chrysanthemum: a review. *Hortic Res*. 2019;6:109. doi:10.1038/s41438-019-0193-8
20. Tymoszuk A, Kulus D. Silver nanoparticles induce genetic, biochemical, and phenotype variation in chrysanthemum. *Plant Cell Tissue Organ Cult*. 2020;143:331–344. doi:10.1007/s11240-020-01920-4
21. Tymoszuk A, Kulus D. Effect of silver nanoparticles on the in vitro regeneration, biochemical, genetic, and phenotype variation in adventitious shoots produced from leaf explants in chrysanthemum. *IJMS*. 2022;23(13):7406. doi:10.3390/ijms23137406
22. Tymoszuk A, Sławkowska N, Szałaj U, et al. Synthesis, characteristics, and effect of zinc oxide and silver nanoparticles on the in vitro regeneration and biochemical profile of chrysanthemum adventitious shoots. *Materials*. 2022;15(22):8192. doi:10.3390/ma15228192
23. Tymoszuk A, Szałaj U, Wojnarowicz J, et al. Zinc oxide and silver effects on the growth, pigment content and genetic stability of chrysanthemums propagated by the node culture method. *Folia Horticult*. 2024;36(1):35–66. doi:10.2478/fhort-2024-0003
24. Ghasempour A, Dehghan H, Ataee M, et al. Cadmium sulfide nanoparticles: preparation, characterization, and biomedical applications. *Molecules*. 2023;28:3857. doi:10.3390/molecules28093857
25. Ullah H, Zheng W, Sheng Y. Translocation of CdS nanoparticles in maize (*Zea mays* L.) plant and its effect on metabolic response. *Chemosphere*. 2023;343:140189. doi:10.1016/j.chemosphere.2023.140189
26. Haider FU, Liqun C, Coulter JA, et al. Cadmium toxicity in plants: impacts and remediation strategies. *Ecotoxicol Environ Saf*. 2021;211:111887. doi:10.1016/j.ecoenv.2020.111887
27. Likus-Cieślik J, Pietrzykowski M, Chodak M. Chemistry of sulfur-contaminated soil substrate from a former frasch extraction method sulfur mine leachate with various forms of litter in a controlled experiment. *Water Air Soil Pollut*. 2018;229(3):71. doi:10.1007/s11270-018-3716-2
28. Salam A, Rehman M, Qi J, et al. Cobalt stress induces photosynthetic and ultrastructural distortion by disrupting cellular redox homeostasis in maize. *Environ Exp Bot*. 2024;217:105562. doi:10.1016/j.envexpbot.2023.105562
29. Pagar T, Ghotekar S, Pagar K, et al. A review on bio-synthesized Co_3O_4 nanoparticles using plant extracts and their diverse applications. *J Chem Rev*. 2019;1(4):260–270. doi:10.33945/SAMI/jcr.2019.4.2
30. Waris A, Din M, Ali A, et al. Green fabrication of Co and Co_3O_4 nanoparticles and their biomedical applications: a review. *Open Life Sci*. 2021;16(1):14–30. doi:10.1515/biol-2021-0003
31. Ogunyemi SO, Xu X, Xu L, et al. Cobalt oxide nanoparticles: an effective growth promoter of *Arabidopsis* plants and nano-pesticide against bacterial leaf blight pathogen in rice. *Ecotoxicol Environ Saf*. 2023;257:114935. doi:10.1016/j.ecoenv.2023.114935
32. Jahani M, Khavari-Nejad RA, Mahmoodzadeh H, et al. Effects of cobalt oxide nanoparticles (Co_3O_4 NPs) on ion leakage, total phenol, antioxidant enzymes activities and cobalt accumulation in *Brassica napus* L. *Not Bot Horti Agrobo*. 2020;48(3):1260–1275. doi:10.15835/nbha48311766
33. Faisal M, Saquib Q, Alatar AA, et al. Cobalt oxide nanoparticles aggravate DNA damage and cell death in eggplant via mitochondrial swelling and NO signaling pathway. *Biol Res*. 2016;49:20. doi:10.1186/s40659-016-0080-9
34. Hu J, Guo H, Li J, et al. Comparative impacts of iron oxide nanoparticles and ferric ions on the growth of *Citrus maxima*. *Environ Pollut*. 2017;221:199–208. doi:10.1016/j.envpol.2016.11.064
35. Wang Y, Wang S, Xu M, et al. The impacts of γ-Fe_2O_3 and Fe_3O_4 nanoparticles on the physiology and fruit quality of muskmelon (*Cucumis melo*) plants. *Environ Pollut*. 2019;249:1011–1018. doi:10.1016/j.envpol.2019.03.119
36. Banijamali S, Feizian M, Bidabadi A, et al. Effect of magnetite nanoparticles on vegetative growth, physiological parameters and iron uptake in chrysanthemum (*Chrysanthemum morifolium*) 'Salvador'. *JOP*. 2019;9:129–142.
37. Kulus D, Tymoszuk A, Gościnna K, et al. Enhancing germination and growth of chrysanthemum synthetic seeds through iron oxide nanoparticles and indole-3-acetic acid: impact of treatment duration on metabolic activity and genetic stability. *Nanotechnol Sci Appl*. 2025;18:139–155. doi:10.2147/NSA.S503868
38. Harish V, Aslam S, Chouhan S, et al. Iron toxicity in plants: a review. *Int J Environ Clim Chang*. 2023;13(8):1894–1900. doi:10.9734/ijecc/2023/v13i82145
39. Dittmer A, da Costa Gouveia TL, Sivalingam K, et al. Revisiting the band gap problem in bulk Co_3O_4 and its isostructural Zn and Al derivatives through the lens of theoretical spectroscopy. *Phys Chem Chem Phys*. 2025;27:17225–17244.
40. Nagamine M, Osial M, Widera-Kalinowska J, et al. Photosensitive thin films based on drop cast and langmuir-blodgett hydrophilic and hydrophobic CdS nanoparticles. *Nanomaterials*. 2020;10:2437. doi:10.3390/nano10122437
41. Alsalmah HA, Aadil M, Zulfiqar S. Eco-engineered Fe-doped Co_3O_4 nanostructures: band gap tuning and surface engineering for environmental remediation. *Ceram Internat*. 2025. doi:10.1016/j.ceramint.2025.08.266
42. Makhlouf SA, Bakr ZH, Aly KI, et al. Structural, electrical and optical properties of Co_3O_4 nanoparticles. *Superlattice Microst*. 2013;64:107–117. doi:10.1016/j.spmi.2013.09.023

43. Rabee AIM, Gaid CBA, Mekhemer GAH, et al. Combined TPR, XRD, and FTIR studies on the reduction behavior of Co_3O_4. *Mater Chem Phys*. 2022;289:236367. doi:10.1016/j.matchemphys.2022.126367
44. Yousif NA, AL-Jawad SMH, Taha AA. Preparation and characterization of pure and Ni/Co–Co-doped Fe_3O_4 nanoparticles and investigation of their in vitro hemolysis effects. *Plasmonics*. 2024;19:2345–2361. doi:10.1007/s11468-023-02167-3
45. Anjum S, Tufail R, Rashid K, et al. Effect of cobalt doping on crystallinity, stability, magnetic and optical properties of magnetic iron oxide nano-particles. *J Magn Magn Mater*. 2017;432:198–207. doi:10.1016/j.jmmm.2017.02.006
46. Khan ZR, Zulfequar M, Khan MS. Chemical synthesis of CdS nanoparticles and their optical and dielectric studies. *J Mater Sci*. 2011;46:5412–5416. doi:10.1007/s10853-011-5481-0
47. Heiba ZK, Mohamed MB, Abdellatief M, et al. Influence of alloying ratio in tailoring the structural and optical properties of (1 − x)CdS–xCuS nanocomposite. *Appl Phys A*. 2020;126:518. doi:10.1007/s00339-020-03700-5
48. Valluvan R, Selvaraju K, Kumararaman S. Growth and characterization of sulphamic acid single crystals: a nonlinear optical material. *Mater Chem Phys*. 2006;97(1):81–84. doi:10.1016/j.matchemphys.2005.07.063
49. Pietrzyk-Thel P, Osial M, Pregowska A, et al. SPIONs doped with cobalt from the Li-ion battery acid leaching waste as a photocatalyst for tetracycline degradation – synthesis, characterization, DFT studies, and antibiotic treatment. *Desalin Water Treat*. 2023;305:155–173. doi:10.5004/dwt.2023.29795
50. Murashige T, Skoog F. A revised medium for rapid growth and bioassays with tobacco tissue cultures. *Physiol Plant*. 1962;15:473–497. doi:10.1111/j.1399-3054.1962.tb08052.x
51. Homaee MB, Ehsanpour AA. Silver nanoparticles and silver ions: oxidative stress responses and toxicity in potato (*Solanum tuberosum* L.) grown in vitro. *Hortic Environ Biotechnol*. 2016;57(6):544–553.
52. Bradford MM. A rapid and sensitive method for the quantitation of microgram quantities of protein utilizing the principle of protein-dye binding. *Anal Biochem*. 1976;72:248–254. doi:10.1016/0003-2697(76)90527-3
53. Nakano Y, Asada K. Hydrogen peroxide is scavenged by ascorbate specific peroxidase in spinach chloroplasts. *Plant Cell Physiol*. 1981;22:867–880. doi:10.1093/oxfordjournals.pcp.a076232
54. Maehly AC, Chance B. The assay of catalases and peroxidases. In: Glick D, editor. *Methods of Biochemical Analysis*. New York: Willey; 1954. doi:10.1002/9780470110171.ch14
55. Nowogórska A, Patykowski J. Selected reactive oxygen species and antioxidany enzymes in common bean after *Pseudomonas syringae* pv. *phaseolicola* and *Botrytis cinerea* infection. *Acta Physiol Plant*. 2015;37:1725. doi:10.1007/s11738-014-1725-3
56. Giannopolitis CN, Ries SK. Superoxide dismutases I. Occurrence in higher plants. *Plant Physiol*. 1977;59:309–314. doi:10.1104/pp.59.2.309
57. Keutgen AJ, Pawelzik E. Modifications of strawberry fruit antioxidant pools and fruit quality under NaCl stress. *J Agric Food Chem*. 2007;55 (10):4066–4072. doi:10.1021/jf070010k
58. Benzie IFF, Strain JJ. The ferric reducing ability of plasma (FRAP) as a measure of "antioxidant power": the FRAP assay. *Analytic Biochem*. 1996;239:70–76. doi:10.1006/abio.1996.0292
59. Re R, Pellegrini N, Proteggente A, et al. Antioxidant activity applying an improved ABTS radical cation decolorization assay. *Free Radic Biol Med*. 1999;26(9/10):1231–1237. doi:10.1016/S0891-5849(98)00315-3
60. RHSCC. *The Royal Horticultural Society Colour Chart*. London; 1966.
61. Harborne JB. Comparative biochemistry of the flavonoids. *Phytochemistry*. 1967;6(11):1569–1573. doi:10.1016/S0031-9422(00)82952-0
62. Williams JGK, Kubelik AR, Livak KJ, et al. DNA polymorphisms amplified by arbitrary primers are useful as genetic markers. *Nucleic Acids Res*. 1990;18:6531–6535. doi:10.1093/nar/18.22.6531
63. Collard BCY, Mackill DJ. Start codon targeted (Scot) polymorphism: a simple, novel DNA marker technique for generating gene-targeted markers in plants. *Plant Mol Biol Rep*. 2009;27:86–93. doi:10.1007/s11105-008-0060-5
64. Peakall R, Smouse PE. GenAlEx 6.5: genetic analysis in Excel. Population genetic software for teaching and research-an update. *Bioinformatics*. 2012;28(19):2537–2539. doi:10.1093/bioinformatics/bts460
65. Amiryousefi A, Hyvönen J, Poczai P. iMEC: online marker efficiency calculator. *Appl Plant Sci*. 2018;6(6):e1159. doi:10.1002/aps3.1159
66. Singh KM, Jha AB, Dubey RS, et al. Nanoparticle-mediated mitigation of salt stress-induced oxidative damage in plants: insights into signaling, gene expression, and antioxidant mechanisms. *Environ Sci: Nano*. 2025;12:2983–3017. doi:10.1039/D5EN00174A
67. Yasur J, Rani P. Environmental effects of nanosilver: impact on castor seed germination, seedling growth, and plant physiology. *Environ Sci Pollut Res*. 2013;20:8636–8648. doi:10.1007/s11356-013-1798-3
68. Thiruvengadam M, Gurunathan S, Chung I-M. Physiological, metabolic, and transcriptional effects of biologically-synthesized silver nano-partciles in turnip (*Brassica rapa* ssp. *rapa* L.). *Protoplasma*. 2015;252:1031–1046. doi:10.1007/s00709-014-0738-5
69. Mcgehee DL, Lahiani MH, Irin F, et al. Multiwalled carbon nanotubes dramatically affect the fruit metabolome of exposed tomato plants. *ACS Appl Materials Interfaces*. 2017;9:32430–32435. doi:10.1021/acsami.7b10511
70. Sieprawska A, Rudolphi-Szydło E, Skórka M, et al. Assessment of the oxidative stress intensity and the integrity of cell membranes under the manganese nanoparticles toxicity in wheat seedlings. *Sci Rep*. 2024;14:3121. doi:10.1038/s41598-024-53697-7
71. Amorati R, Valgimigli L. Methods to measure the antioxidant activity of phytochemicals and plant extracts. *J Agric Food Chem*. 2018;66 (13):3324–3329. doi:10.1021/acs.jafc.8b01079
72. Chaves N, Santiago A, Alías JC. Quantification of the antioxidant activity of plant extracts: analysis of sensitivity and hierarchization based on the method used. *Antioxidants*. 2020;9(1):76. doi:10.3390/antiox9010076
73. Thakur S, Asthir B, Kaur G, et al. Zinc oxide and titanium dioxide nanoparticles influence heat stress tolerance mediated by antioxidant defense system in wheat. *Cereal Res Commun*. 2022;50:385–396. doi:10.1007/s42976-021-00190-w
74. Wei Y, He Y, Wu Y. Soil application of SiNPs suppress pathogen population and improved plant resistance and antioxidant activity for disease management. *S Afr J Bot*. 2024;172:31–41. doi:10.1016/j.sajb.2024.06.049
75. Owji H, Hemmati S, Heidari R, et al. Effect of alumina (Al_2O_3) nanoparticles and macroparticles on *Trigonella foenum-graceum* L. in vitro cultures: assessment of growth parameters and oxidative stress-related responses. *3 Biotech*. 2019;9:419. doi:10.1007/s13205-019-1954-7
76. Modarresi M, Chahardoli A, Karimi N, et al. Variations of glaucine, quercetin and kaempferol contents in *Nigella arvensis* against Al_2O_3, NiO, and TiO_2 nanoparticles. *Heliyon*. 2020;6:e04265. doi:10.1016/j.heliyon.2020.e04265

77. Mohasseli V, Farbood F, Moradi A. Antioxidant defense and metabolic responses of lemon balm (*Melissa officinalis* L.) to Fe-nano-particles under reduced irrigation regimes. *Ind Crops Prod*. 2020;149:112338. doi:10.1016/j.indcrop.2020.112338
78. Rawat M, Yadukrishnan P, Kumar N. Mechanisms of action of nanoparticles in living systems. In: Pankay SA editor. *Microbial Biotechnology in Environmental Monitoring and Cleanup*. IGI Global Scientific Publishing; 2018:220–236. doi:10.4018/978-1-5225-3126-5.ch014
79. Banerjee K, Pramanik P, Maity A, et al. Chapter 4 - Methods of using nanomaterials to plant systems and their delivery to plants (Mode of entry, uptake, translocation, accumulation, biotransformation and barriers). In: Ghorbanpour M, Wani SH, editors. *Advances in Phytonanotechnology*. Academic Press; 2019:123–152. doi:10.1016/B978-0-12-815322-2.00005-5
80. Juárez-Maldonado A. Influence of nanomaterials on non-enzymatic antioxidant defense activities in plants. In: Al-Khayri JM, Alnaddaf LM, Jain SM, editors. *Nanomaterial Interactions with Plant Cellular Mechanisms and Macromolecules and Agricultural Implications*. Cham: Springer; 2023:273–298. doi:10.1007/978-3-031-20878-2_10
81. Boudet AM. Evolution and current status of research in phenolic compounds. *Phytochemistry*. 2007;68:2722–2735. doi:10.1016/j.phytochem.2007.06.012
82. Zoufan P, Baroonian M, Zargar B. ZnO nanoparticles-induced oxidative stress in *Chenopodium murale* L. Zn uptake, and accumulation under hydroponic culture. *ESPR*. 2020;27:11066–11078. doi:10.1007/s11356-020-07735-2
83. Patil SA, Kulkarni AJ, Jadhav PR, et al. Potential assessment of *Chrysanthemum* flowers from various cultivars as sources of natural antioxidants and bioactive compounds. *Genet Resour Crop Evol*. 2025;72:1599–1617. doi:10.1007/s10722-024-02035-x
84. Cao X, Xiong X, Xu Z, et al. Comparison of phenolic substances and antioxidant activities in different varieties of chrysanthemum flower under simulated tea making conditions. *J Food Meas Charact*. 2020;14:1443–1450. doi:10.1007/s11694-020-00394-4
85. Kulus D, Tymoszuk A, Kulpińska A, et al. Synergistic effects of iron oxide nanoparticles and indole-3-acetic acid on the germination and development of cold-stored chrysanthemum synthetic seeds. *Plant Cell Tissue Organ Cult*. 2025;160:18. doi:10.1007/s11240-024-02955-7
86. Rout GR, Sahoo S. Role of iron in plant growth and metabolism. *Rev Agric Sci*. 2015;3:1–24. doi:10.7831/ras.3.1
87. Bajpay A, Dwivedi D. Gamma ray induced foliage variegation and anatomical aberrations in chrysanthemum (*Dendranthema grandiflora* T.) cv. Maghi. *J Pharmacogn Phytochem*. 2019;8(14):874.
88. Zalewska M, Tymoszuk A, Miler N. New chrysanthemum cultivars as a result of in vitro mutagenesis with the applications of different explant types. *Acta Sci Pol, Hortorum Cultus*. 2011;10(2):109–123.
89. Sakamoto W. Leaf-variegated mutations and their responsible genes in *Arabidopsis thaliana*. *Genes Genet Syst*. 2003;78(1):1–9. doi:10.1266/ggs.78.1
90. Yu F, Fu A, Aluru M, et al. Variegation mutants and mechanisms of chloroplast biogenesis. *Plant Cell Environ*. 2007;30(3):350–365. doi:10.1111/j.1365-3040.2006.01630.x
91. Mandal A, Chakrabarty D, Datta S. Application of in vitro techniques in mutation breeding of chrysanthemum. *Plant Cell Tissue Organ Cult*. 2020;60:33–38. doi:10.1023/A:1006442316050
92. Gorji AM, Poczai P, Polgar Z, et al. Efficiency of arbitrarily amplified dominant markers (Scot, ISSR and RAPD) for diagnostic fingerprinting in tetraploid potato. *Am J Pot Res*. 2011;88:226–237. doi:10.1007/s12230-011-9187-2
93. Hromadová Z, Gálová Z, Mikolášová L, et al. Efficiency of RAPD and Scot markers in the genetic diversity assessment of the common bean. *Plants*. 2023;12(15):2763. doi:10.3390/plants12152763
94. Cui D, Wang J, Wang H, et al. The cytotoxicity of endogenous CdS and Cd^{2+} ions during CdS NPs biosynthesis. *J Hazard Mater*. 2021;409:124485. doi:10.1016/j.jhazmat.2020.124485
95. Mohamed HRH, Mohamed BA, Hakeem G, et al. Cobalt oxide nanoparticles induce cytotoxicity and excessive ROS mediated mitochondrial dysfunction and p53-independent apoptosis in melanoma cells. *Sci Rep*. 2025;15:2220. doi:10.1038/s41598-025-85691-y
96. Das R, Mohanty B. Evaluating the toxicological impacts of cobalt, copper, and cadmium on seed germination. *Int J Biol Sci*. 2023;5(2):121–124. doi:10.33545/26649926.2023.v5.i2b.221
97. Haspolat G. Variations in flower color of mutant chrysanthemums. *Horticulturae*. 2024;10(4):385. doi:10.3390/horticulturae10040385
98. Din A, Qadri ZA, Wani MA, et al. Comparative analysis of physical and chemical mutagenesis in chrysanthemum cv. 'Candid': assessing genetic variation and breeding potential. *ACS Omega*. 2023;8(46):43836–43849. doi:10.1021/acsomega.3c05723
99. Begum T, Dasgupta T. A comparison of the effects of physical and chemical mutagens in sesame (*Sesamum indicum* L.). *Genet Mol Biol*. 2010;33(4):761–766. doi:10.1590/S1415-47572010005000090
100. Shahwar D, Khan Z, M.k A, et al. Relative mutagenic effectiveness and efficiency of chemical mutagens (Caffeine and EMS) and heavy metals [$(Pb(NO_3)_2$ and $Cd(NO_3)_2)$] in developing chlorophyll and morphological mutants in lentil. *MRGTEM*. 2023;890:503668. doi:10.1016/j.mrgentox.2023.503668